Meteoritics & Planetary Science 37, 1865–1891 (2002)
Available online at http://www.uark.edu/meteor

The trapped noble gas component in achondrites

HENNER BUSEMANN* AND OTTO EUGSTER

University of Bern, Physics Institute, Sidlerstrasse 5, 3012 Bern, Switzerland
*Correspondence author's e-mail address: busemann@phim.unibe.ch

(Received 2002 June 7; accepted in revised form 2002 September 12)

Abstract–The trapped noble gases Ar, Kr and Xe in several achondrites were analysed. We chose separates of the lodranites Lodran and Graves Nunataks 95209 and bulk samples of the Tatahouine diogenite, Pasamonte eucrite, five aubrites and two angrites. Among these, Lodran, Tatahouine, Pasamonte and the aubrite Norton County have been reported to contain U-Xe, a noble gas component assumed to be the most primitive component in the solar system. U-Xe might have been incorporated into the early Earth. We found large concentrations of Xe in several separates of the Lodran lodranite, however, none of the measurements revealed U-Xe composition. The Xe composition of all achondrites can straightforwardly be explained with mixtures of trapped common Xe-Q, absorbed air and various amounts of fissiogenic and cosmogenic Xe. Reanalysis of literature data for Pasamonte, Angra dos Reis and some aubrites is consistent with Xe-Q as the trapped endmember component and contributions of fissiogenic Xe. The presence of Xe-Q in many primitive achondrites is in agreement with the formation of their parent bodies from originally chondritic precursor material. The Ar-Xe elemental composition of Lodran and the aubrites indicate subsolar composition, which is commonly found in E chondrites. This result supports a model of formation of the aubrites from E-chondritic precursor material.

INTRODUCTION

The analysis of noble gases is an important approach to decipher evolutionary mechanisms in the solar system. Understanding the elemental and isotopic composition of reservoirs such as the Sun, atmospheres and interiors of the planets, comets, interplanetary dust particles and the components found in meteorites leads to a better knowledge of the processes that have formed and altered the bodies of the early solar system.

Whereas non-volatile elements occur in solar abundances in primitive chondrites, the most volatile elements including all noble gases are largely depleted in meteorites (Palme and Beer, 1993). The isotopic composition of the noble gases in meteorites is distinct from those of the Sun, as measured in the solar wind, and the atmospheres and interiors of the planets (Wieler, 2002). Many models deal with the composition of noble gases in planets and the putative relation to solar, meteoritic or cometary noble gases (*e.g.*, Igarashi, 1995; Owen *et al.*, 1992, 1999; Pepin, 1992, 2000; Porcelli and Pepin, 2000; Zahnle, 1993). The nine stable xenon isotopes allow the recognition of radiogenic and fissiogenic contributions that might have accumulated since the formation of a planetary body, and the determination of the fractionation that might have occurred during gas trapping or loss (*e.g.*, from primary atmospheres). The initially incorporated Xe isotopic composition in the Earth is essential to determine the amounts of radiogenic ^{129}Xe and fissiogenic $^{131-136}$Xe that originate from the β-decay of extinct ^{129}I and fission of ^{238}U or extinct ^{244}Pu. These numbers might help to constrain the timing of an early (catastrophic?) outgassing event, the closure time for Xe and the formation interval of the Earth (*e.g.*, Ozima and Podosek, 2002; Porcelli and Pepin, 2000, and references therein).

However, the isotopic composition of the primordial (*i.e.*, non-radiogenic and unfractionated) terrestrial Xe is not known. Neon and possibly Ar in the terrestrial mantle are solar like (Porcelli and Pepin, 2000). Starting accordingly with solar wind Xe as initial terrestrial Xe, processes such as hydrogen-driven hydrodynamic escape would lead to the observed terrestrial atmospheric Xe, except for the isotopes ^{134}Xe and ^{136}Xe, which would be overabundant relative to the observed atmospheric abundances (Porcelli and Pepin, 2000). To account for the contributions of fissiogenic and radiogenic Xe from the Earth's interior, a primordial Xe composition ("U-Xe"—U stands for "Ur", a German word for indigenous) depleted in ^{129}Xe, ^{134}Xe and ^{136}Xe has been suggested (Pepin and Phinney, 1978). The isotopic composition was obtained by analysing in a sophisticated manner the Xe compositions in meteorites, the Sun and the terrestrial atmosphere. Interestingly, this particular Xe isotopic composition has been independently deduced earlier by extrapolation of Xe data in carbonaceous chondrites and achondrites, respectively (Takaoka, 1972). Suggesting that this composition is the original unaltered composition of the trapped

Prelude preprint MS#4856

noble gases in all stony meteorites, Takaoka named it "primitive Xe". The isotopic compositions of "primitive Xe" and "U-Xe" are given in Table 1. Acknowledging the first determination of primitive Xe by Takaoka, we will nevertheless solely use the expression U-Xe, because it has become more common.

Pure U-Xe composition has never been detected. However, some experimental results indicate the possible presence of U-Xe—in combination with other components—in meteorites of different classes. Takaoka's determination of U-Xe is based on the literature data of the aubrite Norton County, the eucrite Pasamonte and the H5 chondrite Achilles (Pasamonte: Hohenberg *et al.*, 1967; Norton County: Munk, 1967; Achilles: Rowe *et al.*, 1965). Pepin and Phinney used a large data set obtained by stepwise heating of Pasamonte (Hohenberg *et al.*, 1967) and the Angra dos Reis angrite (Hohenberg, 1970) to confirm their endmember composition of U-Xe. Other experimental evidence is rare: xenon isotopic data for some temperature steps of the diogenite Tatahouine and mineral separates of Lodran indicate U-Xe (Michel and Eugster, 1994; Weigel and Eugster, 1994). Xenon in acid-resistant residues of the IAB iron meteorite El Taco has been explained by a mixture of fractionated U-Xe and fission Xe (Mathew and Begemann, 1995). Silicates in the Brenham pallasite might contain U-Xe or solar wind Xe (Nagao and Miura, 1994). A low-temperature step of the CM2 chondrite Murray seems to indicate U-Xe in the heavier isotopes (Niemeyer and Zaikowski, 1980) and Xe isotope correlations found in etched samples of this meteorite lead to U-Xe composition (Jones *et al.*, 1985). Finally, Mahaffy *et al.* (2000) found the Xe isotopic composition of the jovian atmosphere to be in agreement with U-Xe. However, depending on the normalising isotope (^{130}Xe or ^{132}Xe), the data are within their large uncertainties (revised in Wieler, 2002) similarly consistent with solar or meteoritic composition (Wieler, 2002).

It appears surprising that hints at the most primitive Xe composition in the solar system were mostly found in achondrites rather than in the less evolved chondrites. In the following, we thus want to address the question of the composition of the trapped heavy noble gases in achondrites and its relationship to common chondritic components. We discuss new measurements of the Ar, Kr and Xe isotopic and elemental composition in bulk samples and separates of those achondrites that have been reported to contain U-Xe. Additionally, data for four other aubrites and two angrites are presented. Furthermore, we reevaluate the analyses of the trapped Xe composition in achondrites of previous studies. Here, we will not discuss the composition of the noble gases in ureilites, the second largest group of achondrites, because of the similarity of the ureilitic noble gases with the Q-gases (see, for example, Ott, 2002, and references therein). Preliminary results of this work were published in abstracts (Busemann and Eugster, 2000a,b). Cosmic-ray exposure ages of the aubrites and the excesses of $^{80/82}$Kr due to the enhanced flux of epithermal neutrons on the aubrite parent body are discussed in more detail by Lorenzetti *et al.* (2002).

TABLE 1. The Xe isotopic composition of primitive Xe, U-Xe, Xe-Q and the average of gas-rich separates of Lodran.

	^{124}Xe/^{130}Xe	^{126}Xe/^{130}Xe	^{128}Xe/^{130}Xe	^{129}Xe/^{130}Xe	^{131}Xe/^{130}Xe	^{132}Xe/^{130}Xe	^{134}Xe/^{130}Xe	^{136}Xe/^{130}Xe	Reference
Primitive Xe	(2.951)	(2.623)	$50.8^{+5.5}_{-1.8}$	–	490^{+33}_{-14}	595^{+38}_{-16}	211^{+11}_{-4}	$163.9^{+8.1}_{-2.7}$	Takaoka (1972)
U	2.928 ± 0.010	2.534 ± 0.013	50.83 ± 0.06	628.6 ± 0.6	499.6 ± 0.6	604.7 ± 0.6	212.6 ± 0.4	165.7 ± 0.3	Pepin (2000)
Lodran separates, average*	2.76 ± 0.04	2.492 ± 0.026	50.44 ± 0.29	645.1 ± 2.5	502.5 ± 1.0	608.7 ± 1.1	228.5 ± 1.2	191.5 ± 0.5	This work
Q	2.810 ± 0.016	2.505 ± 0.013	50.78 ± 0.17	643.7 ± 1.8	505.4 ± 1.2	617.5 ± 1.3	233.4 ± 0.8	195.4 ± 0.7	Busemann *et al.* (2000)
Air	2.337 ± 0.007	2.180 ± 0.011	47.15 ± 0.07	649.6 ± 0.9	521.3 ± 0.8	660.7 ± 0.5	256.3 ± 0.4	217.6 ± 0.3	Basford *et al.* (1973)

See also Fig. 4. (^{130}Xe ≡ 100).
*Average of the six major steps with ^{132}Xe concentrations >800 × 10^{-12} cm^3/g (see Table 3).

EXPERIMENTAL PROCEDURE AND SAMPLE PREPARATION

All samples (Table 2) were analysed, wrapped in ~100 mg Ni foil, in a Mass Analyser Products 215-50 mass spectrometer equipped with an Ortec type 9xx counting system. We measured several samples at 500–600 °C to release possible air contamination separately, the major step at 1700 °C, and additionally at 1730–1800 °C to check the completeness of the gas extraction. Only the major steps of three metal-rich Lodran samples and four Millbillillie aliquots did not reach complete degassing at 1700 °C. In these few cases, the ^{132}Xe concentrations given in Tables 3 and A3 include the respective ^{132}Xe concentrations of the re-extraction steps (2–17% of the major release). One of the Fe/Ni-rich fractions of Lodran as well as the silicate-rich fraction of Lodran and the Fe/Ni-rich fraction of Graves Nunataks (GRA) 95209 were measured at stepwise increasing temperatures between 500 and 1750 °C to resolve possible compositional differences and to allow a comparison of our results with earlier work (Weigel and Eugster, 1994). Tatahouine was also measured stepwise, similar to the measurements of Michel and Eugster (1994). We performed fewer steps than in the previous experiment in order to improve the counting statistics. The gases, extracted in an all-molybdenum crucible, were separated in Ar, Kr and Xe-rich fractions with activated charcoal at temperatures of –196, –40 and +40 °C, respectively. Performance and linearity of the digital system during the 2.5 years of measurements were checked with 100–500 mg of our laboratory standard sample (splits of the Millbillillie eucrite crushed to <750 μm). The new results are in agreement with each other (standard deviation of the means of the isotopic ratios mainly <1% for Xe and <2% for Kr, although terrestrial contaminations largely vary) and do not show systematic deviations from measurements performed earlier in our institute with the analogue technique or with results given in the literature (Tables A1–A3 in the appendix). The uncertainty of the sensitivity is assumed to be <15%. Mass fractionation was determined by measuring Kr and Xe in (80–500) $\times 10^{-8}$ cm^3 of air. Relative to the isotopic composition for Kr_{air} and Xe_{air} given by Basford *et al.* (1973), the average mass fractionation for the Kr and Xe isotopic ratios range between 0.2 and 0.9‰/amu. The standard deviations of the respective mass fractionation of <35% are included in the uncertainties. Argon was measured with the Faraday cup. The measurement of the $^{40}Ar/^{36}Ar$ ratio in air gave an average mass fractionation of 0.0 ± 0.3%/amu which was adopted for $^{36}Ar/^{38}Ar$. The Ar sensitivity depends on the total gas amount and was determined with standard amounts of Ar comparable to the Ar amounts in the samples, whereas the Kr and Xe measurements of air did not yield significant non-linearity of the sensitivity. The extraction temperature is assumed to be correct within ±150 K at low and ±50 K at high temperatures. Finally, the extracted gases were cleaned with Ti at temperatures of 700 °C cooled down to ~300 °C, which was replaced in more recent measurements by SAES ST101 pellets at 280 and 400 °C, and a SAES GP50 getter. Blanks were determined by measuring Ni foils at appropriate temperatures and typically amount to (in 10^{-12} cm^3 STP): ^{36}Ar = 30, ^{84}Kr = 0.3 and ^{132}Xe = 0.2. This normally contributes to <4, 10 and 5%, respectively, of the released ^{36}Ar, ^{84}Kr and ^{132}Xe. Corrections exceeding these typical numbers by more than a factor of 2 are marked in the tables. The uncertainties (1σ) of the absolute concentrations given in the tables include corrections for the amounts measured in the other gas fractions, blanks and statistics. Uncertainties of the isotopic ratios (1σ) include statistics, mass fractionation and blank corrections. Most bulk samples were not crushed in order to reduce air contamination. The lodranite separates were crushed to a grain size <750 μm, separated with a magnet and finally handpicked (Table 2). A few metal-rich grains of Lodran were etched for different periods in concentrated HF (Table 2).

RESULTS

The results are given in Tables 3–5 and A1–A3. All data indicate mixtures of primordially trapped (tr), cosmogenic (cosm), radiogenic (rad), fissiogenic (fiss) and atmospheric noble gases. As a first step, we subtracted the cosmogenic contributions. We used $(^{36}Ar/^{38}Ar)_{cosm} = 0.65 \pm 0.02$ (adopted from achondrite data in Schultz and Kruse, 2000) and both $(^{36}Ar/^{38}Ar)_{tr} = 5.26$ and 5.39 to obtain the $^{36}Ar_{tr}$ concentrations (Tables 4 and A1). The uncertainty of $^{36}Ar_{tr}$ covers both choices. The values chosen for Ar_{tr} includes air and Q (Busemann *et al.*, 2000) but not solar Ar, because the He and Ne compositions do not indicate the presence of solar wind in the samples (Lorenzetti *et al.*, 2002; Michel and Eugster, 1994; Terribilini *et al.*, 2000; Weigel *et al.*, 1999). The calculated $^{36}Ar_{tr}$ is considerably uncertain because the cosmogenic ^{36}Ar often amounts to almost 100% of the measured ^{36}Ar (Tables 4 and A1).

Cosmogenic Kr was corrected for *via* $^{86}Kr/^{83}Kr$, assuming the trapped Kr to be air or Kr-Q (Busemann *et al.*, 2000). The uncertainty of $^{83}Kr_{cosm}$ covers both choices of the trapped component. The cosmogenic production of ^{86}Kr is not very well known. We adopted the range $(^{86}Kr/^{83}Kr)_{cosm} = 0–0.015$ (Marti *et al.*, 1966; Marti and Lugmair, 1971). For the other ratios $(^{x}Kr/^{83}Kr)_{cosm}$ we used the composition determined by Marti *et al.* (1966) in the eucrite Stannern. For the aubrites and angrites we determined new sets of average cosmogenic Kr ratios according to the method described in Table A4 in the appendix, acknowledging that especially the $(^{78}Kr/^{83}Kr)_{cosm}$ ratio strongly depends on the depths of the samples within the meteoroids (*e.g.*, Eugster *et al.*, 1969). The resulting concentrations of $^{84}Kr_{tr}$ are given in Tables 5 and A2.

The corrections for Xe_{cosm} are essential in order to obtain pure Xe_{tr} isotopic ratios in achondrites. Therefore, we discuss here the corrections in more detail. We had to correct our aubrite, angrite and Pasamonte data as well as the bulk literature data for Pasamonte, Angra dos Reis and the aubrites except for

TABLE 2. Sample selection and temperature steps.

Sample	Number		Mass (mg)*	Temperature steps (°C)†	Label‡
Tatahouine	BE-349§	Bulk	1282.64	**800, 1400, 1700**, 1800	Ta 8, 14, 17
	BE-559	Bulk chunks	1010.30	**800, 1400, 1700**, 1800	Ta chu 8, 14, 17
	BE-559	Bulk <750 μm	998.02	**800, 1400, 1700**, 1800	Ta pow 8, 14, 17
Lodran	BE-551	Fe/Ni-rich grains, magnetically separated	13.37	**1700**, 1730	Lo BE551 Fe/Ni
	BE-555	Fe/Ni-rich grains, magnetically separated	14.24	**1700**, 1800	Lo Fe/Ni
	BE-555	Fe/Ni-rich grain, dissolved for 2.5 h in HF	0.92	**1700**, 1750	Lo Fe/Ni 2.5 h HF
	BE-555	Fe/Ni-rich grains, magnetically separated	41.69	500, **1000, 1200, 1400, 1600**, 1750	Lo Fe/Ni 10, 12, 14, 16
	BE-555	Fe/Ni-rich grain, dissolved for 10 min in HF	8.32	**1700**, 1750	Lo Fe/Ni 10 m HF
	BE-555	Handpicked troilite-rich grains	18.21	**1700**, 1750	Lo FeS
	BE-555	Fe/Ni-rich grain, dissolved for 40 min in HF	14.69	**1700**, 1750	Lo Fe/Ni 40 m HF
	BE-555	Handpicked silicate-rich grains	48.26	600, **1000, 1200, 1400, 1600**, 1750	Lo Si 10, 12, 14, 16
Graves Nunataks 95209	BE-555	Fe/Ni-rich grains, magnetically separated	54.24	600, **1000, 1200, 1400, 1600**, 1750	GRA 10, 12, 14, 16
Norton County I	BE-161	Bulk	96.22	500, **1700**, 1750	NC I
Norton County II	BE-161	Bulk	204.66	600, 800, **1700**, 1750	NC II
Cumberland Falls	BE-275	Bulk	71.11	500, **1700**, 1750	CF
Mount Egerton	BE-621	Bulk	84.38	500, **1700**, 1750	ME
Mayo Belwa	BE-573	Bulk	82.53	600, **1600**, 1750	MB
Shallowater	BE-265	Bulk	82.84	600, **1600**, 1750	SW
Pasamonte	BE-81	Bulk	92.39	600, **1700**, 1740	PM
Millbillillie #1	BE-531	Bulk <750 μm	512.20	**1700**, 1730	#1
Millbillillie #2	BE-531	Bulk <750 μm	100.28	**1700**, 1730	#2
Millbillillie #3	BE-531	Bulk <750 μm	205.08	**1700**, 1800	#3
Millbillillie #4	BE-531	Bulk <750 μm	432.70	**1700**, 1730	#4
Millbillillie #5	BE-531	Bulk <750 μm	431.24	**1700**, 1740	#5
Millbillillie #6	BE-531	Bulk <750 μm	440.62	**1700**	#6
Millbillillie #7	BE-531	Bulk <750 μm	396.27	**1700**, 1750	#7
Millbillillie #8	BE-531	Bulk <750 μm	420.12	**1700**, 1750	#8
Millbillillie #9	BE-531	Bulk <750 μm	420.08	**1700**, 1750	#9
Millbillillie #10	BE-531	Bulk <750 μm	385.80	**1700**, 1750	#10
Millbillillie #11	BE-531	Bulk <750 μm	490.15	**1700**, 1750	#11
Millbillillie #12	BE-531	Bulk <750 μm	451.40	**1700**, 1750	#12
Millbillillie #13	BE-531	Grinded oxidized crust	436.43	**1700**, 1750	#13
Sahara 99555	BE-707	Bulk	170.31	600, **1700**, 1750	Sa
D'Orbigny	BE-724	Bulk	378.91	600, **1700**, 1750	D'O

*Uncertainty assumed to be ±0.10 mg, Millbillillie #10: ±0.30.
†Major steps in bold letters.
‡Used in the figures, only major steps are considered.
§Bern meteorite collection number.

TABLE 3. Xe concentrations and isotopic composition in bulk achondrites and mineral-rich separates of Lodran and Graves Nunataks 95209.

	^{132}Xe ($^{132}Xe_{tr}$) (10^{-12} cm^3/g)	$^{124}Xe/^{132}Xe$	$^{126}Xe/^{132}Xe$	$^{128}Xe/^{132}Xe$	$^{129}Xe/^{132}Xe$	$^{130}Xe/^{132}Xe$	$^{131}Xe/^{132}Xe$	$^{134}Xe/^{132}Xe$	$^{136}Xe/^{132}Xe$	$^{126}Xe_{cosm}$ (10^{-12} cm^3/g)	$^{136}Xe_f$*
Tatahouine 800 °C†	0.84 ± 0.07	0.35 ± 0.06	0.31 ± 0.06	7.3 ± 1.0	103 ± 14	15.1 ± 2.1	80 ± 11	36 ± 5	32 ± 5	b.d.	b.d.
Tatahouine 1400 °C†	0.77 ± 0.06	0.32 ± 0.06	0.31 ± 0.08	6.7 ± 1.1	97 ± 14	15.2 ± 2.2	80 ± 11	37 ± 5	34 ± 5	b.d.	b.d.
Tatahouine†	0.46 ± 0.06	0.43 ± 0.13	0.44 ± 0.13	7.1 ± 1.7	98 ± 22	18 ± 4	80 ± 18	42 ± 9	36 ± 8	b.d.	b.d.
Tatahouine chunks 800 °C	1.04 ± 0.03	0.334 ± 0.019	0.31 ± 0.03	7.77 ± 0.27	96 ± 4	13.9 ± 0.6	75.2 ± 2.5	38.1 ± 1.2	31.6 ± 1.1	b.d.	b.d.
Tatahouine chunks 1400 °C	12.0 ± 0.4	0.353 ± 0.014	0.331 ± 0.020	7.04 ± 0.21	96.7 ± 1.3	15.4 ± 0.2	79.2 ± 0.9	38.2 ± 0.4	32.8 ± 0.5	b.d.	b.d.
Tatahouine chunks	3.40 ± 0.09	0.343 ± 0.016	0.336 ± 0.011	7.33 ± 0.23	97.9 ± 2.7	15.0 ± 0.4	80.1 ± 2.4	38.6 ± 1.2	32.0 ± 1.0	b.d.	b.d.
Tatahouine powder 800 °C†	0.099 ± 0.006	0.29 ± 0.08	0.46 ± 0.10	6.4 ± 0.7	104 ± 7	17.8 ± 1.0	77 ± 5	39.1 ± 2.9	33.9 ± 2.1	0.00009 ± 0.00009	b.d.
Tatahouine powder 1400 °C†	1.06 ± 0.11	0.32 ± 0.04	0.29 ± 0.04	6.2 ± 0.7	98 ± 10	13.7 ± 1.6	70 ± 8	35 ± 4	35 ± 4	b.d.	b.d.
Tatahouine powder†	0.43 ± 0.06	0.45 ± 0.06	0.54 ± 0.07	6.7 ± 1.1	106 ± 14	14.0 ± 2.3	86 ± 12	38 ± 6	33 ± 5	0.00093 ± 0.00012	b.d.
Norton County I†	7.7 (7.6) ± 1.2	1.63 ± 0.17	2.36 ± 0.19	10.4 ± 0.5	103 ± 4	16.8 ± 0.7	80.3 ± 2.8	38.2 ± 1.4	33.0 ± 1.3	0.1538 ± 0.0025	b.d.
Norton County II†	10.8 (10.7) ± 1.0	1.39 ± 0.06	1.98 ± 0.12	10.1 ± 0.6	104 ± 6	15.5 ± 1.0	83 ± 6	40.9 ± 2.6	34.1 ± 2.1	0.176 ± 0.005	b.d.
Cumberland Falls	117 ± 8	0.511 ± 0.013	0.505 ± 0.015	9.10 ± 0.10	149.1 ± 1.0	16.38 ± 0.16	83.0 ± 0.4	38.0 ± 0.3	31.9 ± 0.3	0.13 ± 0.04	b.d.
Mount Egerton	14.7 ± 1.6	0.37 ± 0.04	0.34 ± 0.05	6.18 ± 0.19	99.0 ± 1.7	15.7 ± 0.4	80.3 ± 1.5	38.8 ± 0.8	32.2 ± 0.8	b.d.	b.d.
Mayo Belwa 1600 °C	20.6 (20.5) ± 0.5	0.88 ± 0.05	1.20 ± 0.07	8.57 ± 0.24	106.3 ± 2.7	16.3 ± 0.6	82.2 ± 2.1	37.7 ± 1.0	31.8 ± 0.8	0.171 ± 0.006	b.d.
Shallowater 1600 °C	551 ± 7	0.448 ± 0.009	0.407 ± 0.007	8.21 ± 0.13	205.8 ± 1.9	16.32 ± 0.18	82.9 ± 0.8	38.2 ± 0.4	32.1 ± 0.4	b.d.	b.d.
Pasamonte†	12.2 ± 1.3 (7.7 ± 1.8)	2.14 ± 0.12	3.27 ± 0.11	8.1 ± 0.6	76 ± 7	12.5 ± 1.1	61 ± 6	65 ± 3	65.0 ± 2.5	0.375 ± 0.006	5.6 ± 1.0
Lodran BE-551 Fe/Ni-rich-rich	**2393 ± 121**	0.419 ± 0.010	0.406 ± 0.013	8.07 ± 0.13	103.7 ± 1.6	16.36 ± 0.29	82.2 ± 1.1	38.2 ± 0.6	31.5 ± 0.5	b.d.	b.d.
Lodran Fe/Ni-rich-rich	538 ± 35	0.40 ± 0.03	0.394 ± 0.028	8.2 ± 0.6	103 ± 7	16.1 ± 1.1	82 ± 6	38.6 ± 2.7	31.6 ± 2.3	b.d.	b.d.
Lodran Fe/Ni-rich 2.5 h HF†	469 ± 68	b.d.	b.d.	7.5 ± 0.7	107 ± 6	15.8 ± 1.3	77 ± 5	38.3 ± 2.6	33.6 ± 2.3	b.d.	b.d.
Lodran Fe/Ni-rich 1000 °C	5.5 ± 0.8	b.d.	b.d.	9.2 ± 0.8	114 ± 4	16.3 ± 0.9	80.6 ± 2.9	38.1 ± 1.5	32.7 ± 1.4	b.d.	b.d.
Lodran Fe/Ni-rich 1200 °C	67 ± 4	0.414 ± 0.023	0.390 ± 0.021	8.26 ± 0.14	107.1 ± 1.0	16.89 ± 0.23	81.5 ± 0.9	37.5 ± 0.5	31.7 ± 0.3	b.d.	b.d.
Lodran Fe/Ni-rich 1400 °C	**1457 ± 63**	0.453 ± 0.007	0.409 ± 0.008	8.30 ± 0.06	106.8 ± 0.6	16.47 ± 0.15	82.9 ± 0.5	37.53 ± 0.22	31.45 ± 0.25	b.d.	b.d.
Lodran Fe/Ni-rich 1600 °C	81 ± 4	0.43 ± 0.03	0.40 ± 0.04	8.40 ± 0.20	107.7 ± 2.0	17.0 ± 0.4	85.2 ± 1.7	37.4 ± 1.0	32.6 ± 0.6	b.d.	b.d.
Lodran Fe/Ni-rich 10 min HF	**1133 ± 61**	0.468 ± 0.012	0.411 ± 0.011	8.40 ± 0.09	106.2 ± 0.9	16.48 ± 0.17	82.1 ± 0.6	37.4 ± 0.3	31.87 ± 0.28	b.d.	b.d.
Lodran troilite-rich	**1849 ± 66**	0.455 ± 0.007	0.394 ± 0.007	8.46 ± 0.07	107.1 ± 0.6	16.50 ± 0.15	83.0 ± 0.5	37.10 ± 0.24	31.4 ± 0.3	b.d.	b.d.
Lodran Fe/Ni-rich 40 min HF	**1591 ± 77**	0.466 ± 0.009	0.423 ± 0.007	8.29 ± 0.12	106.3 ± 1.5	16.3 ± 0.3	82.6 ± 1.2	37.5 ± 0.5	31.5 ± 0.5	b.d.	b.d.
Lodran silicate-rich 1000 °C	19.7 ± 0.8	0.50 ± 0.05	0.37 ± 0.06	6.8 ± 0.3	185 ± 6	15.3 ± 0.7	78 ± 3	36.7 ± 1.8	31.7 ± 1.5	b.d.	b.d.
Lodran silicate-rich 1200 °C	15.0 ± 0.4	0.34 ± 0.05	0.35 ± 0.07	7.6 ± 0.4	127.7 ± 2.8	16.0 ± 0.5	85.1 ± 2.4	38.6 ± 1.1	31.2 ± 0.7	b.d.	b.d.
Lodran silicate-rich 1400 °C	**813 ± 9**	0.460 ± 0.011	0.412 ± 0.007	8.20 ± 0.07	105.8 ± 0.5	16.43 ± 0.12	82.5 ± 0.3	37.53 ± 0.21	31.55 ± 0.24	b.d.	b.d.
Lodran silicate-rich 1600 °C	130.1 ± 2.3	0.484 ± 0.026	0.47 ± 0.03	8.18 ± 0.24	115 ± 4	16.0 ± 0.6	82.5 ± 2.2	36.7 ± 0.9	31.9 ± 1.1	0.11 ± 0.05	b.d.
GRA 95209 Fe/Ni-rich 1000 °C	101.2 ± 1.6	0.369 ± 0.013	0.304 ± 0.011	7.15 ± 0.12	127.9 ± 1.1	15.04 ± 0.16	77.2 ± 0.7	38.2 ± 0.6	32.7 ± 0.4	b.d.	b.d.
GRA 95209 Fe/Ni-rich 1200 °C	17.5 ± 0.3	0.36 ± 0.05	0.43 ± 0.06	7.57 ± 0.22	1554 ± 14	14.5 ± 0.4	82.3 ± 1.2	37.5 ± 0.6	31.0 ± 0.7	0.14 ± 0.07	b.d.
GRA 95209 Fe/Ni-rich 1400 °C	23.6 ± 0.5	0.40 ± 0.03	0.425 ± 0.026	8.66 ± 0.26	279 ± 4	16.2 ± 0.5	80.6 ± 1.8	38.3 ± 0.8	31.4 ± 0.8	b.d.	b.d.
GRA 95209 Fe/Ni-rich 1600 °C	21.0 ± 0.7	0.45 ± 0.04	0.47 ± 0.06	8.51 ± 0.26	179 ± 4	16.8 ± 0.5	86.8 ± 2.4	36.9 ± 1.2	34.6 ± 1.1	0.14 ± 0.09	b.d.

Isotopic ratios normalised to ^{132}Xe = 100. Concentrations in bold letters used to determine Lodran separate average (see Table 1).

*Based on ^{130}Xe, large uncertainties because we used $(^{136}Xe/^{130}Xe)_{tr}$ with an uncertainty that covers U, air and Q composition.

†Blank correction >10% of the measured ^{132}Xe.

Abbreviations: GRA = Graves Nunataks, b.d. = below detection limit.

TABLE 4. Ar concentrations and isotopic composition in bulk achondrites and mineral-rich separates of Lodran and Graves Nunataks 95209.

	^{40}Ar (10^{-8} cm^3/g)	$^{36}Ar/^{38}Ar$	$^{40}Ar/^{36}Ar$	$^{36}Ar_{tr}$ (10^{-8} cm^3/g)	$^{38}Ar_{cosm}$ (10^{-8} cm^3/g)
Tatahouine 800 °C*	1.75 ± 0.06	6.2 ± 0.5†	301 ± 15	0.0059 ± 0.0003	b.d.
Tatahouine 1400 °C	4.65 ± 0.13	0.850 ± 0.010	171.3 ± 2.7	0.0073 ± 0.0011	0.03058 ± 0.00015
Tatahouine‡	2.67 ± 0.08	0.642 ± 0.004	9.31 ± 0.11	b.d.	0.4470 ± 0.0020
Tatahouine chunks 800 °C*	1.86 ± 0.07	4.7 ± 0.3	305 ± 8	0.00598 ± 0.00028	0.000176 ± 0.000016
Tatahouine chunks 1400 °C	27.4 ± 1.2	1.04 ± 0.04	169 ± 4	0.069 ± 0.009	0.1428 ± 0.0008
Tatahouine chunks	13.2 ± 0.5	0.684 ± 0.007	39.9 ± 0.3	0.019 ± 0.017	0.4794 ± 0.0021
Tatahouine powder 800 °C*	0.62 ± 0.03	6.9 ± 2.5	323 ± 21	0.00197 ± 0.00016	b.d.
Tatahouine powder 1400 °C	6.0 ± 0.7	0.75 ± 0.04	92 ± 3	0.010 ± 0.008	0.0841 ± 0.0004
Tatahouine powder	2.31 ± 0.12	0.634 ± 0.003	7.24 ± 0.06	b.d.	0.5050 ± 0.0022
Norton County I	1047 ± 103	0.95 ± 0.04	908 ± 30	0.41 ± 0.12	1.140 ± 0.006
Norton County II	665 ± 302	1.42 ± 0.10	335 ± 14	1.2 ± 0.9	1.165 ± 0.008
Cumberland Falls	1075 ± 115	2.1 ± 0.4	367 ± 16	2.3 ± 0.3	0.925 ± 0.010
Mount Egerton	390 ± 6	1.857 ± 0.023	379 ± 6	0.762 ± 0.025	0.411 ± 0.004
Mayo Belwa 1600 °C	1543 ± 332	1.0 ± 0.3	1527 ± 279	0.42 ± 0.29	0.901 ± 0.005
Shallowater 1600 °C	1027 ± 125	5.42 ± 0.09	42.7 ± 0.5	24.1 ± 2.9	b.d.
Pasamonte	1345 ± 167	0.66 ± 0.10	2131 ± 53	b.d.	0.948 ± 0.004
Lodran BE-551 Fe/Ni-rich-rich	118 ± 6	4.97 ± 0.03	1.468 ± 0.018	80 ± 4	1.22 ± 0.21
Lodran Fe/Ni-rich-rich	55 ± 4	4.75 ± 0.04	2.339 ± 0.029	23.1 ± 1.6	0.60 ± 0.06
Lodran Fe/Ni-rich 2.5 h HF*	b.d.	5.2 ± 0.6	b.d.	14 ± 13	0.05 ± 0.04
Lodran Fe/Ni-rich 1000 °C*	7.7 ± 2.1	2.38 ± 0.29	70 ± 4	0.091 ± 0.030	0.0289 ± 0.0004
Lodran Fe/Ni-rich 1200 °C	2.1 ± 2.0	3.56 ± 0.07	1.209 ± 0.019	b.d.	0.181 ± 0.005
Lodran Fe/Ni-rich 1400 °C	2.3 ± 2.0	5.11 ± 0.04	0.0797 ± 0.0010	28 ± 26	0.26 ± 0.07
Lodran Fe/Ni-rich 1600 °C	b.d.	1.51 ± 0.03	b.d.	b.d.	0.3324 ± 0.0025
Lodran Fe/Ni-rich 10 min HF	34 ± 28	4.78 ± 0.04	0.621 ± 0.008	53 ± 44	1.32 ± 0.15
Lodran troilite-rich	b.d.	4.75 ± 0.07	b.d.	b.d.	0.70 ± 0.07
Lodran Fe/Ni-rich 40 min HF	b.d.	4.79 ± 0.03	b.d.	29 ± 16	0.69 ± 0.08
Lodran silicate-rich 1000 °C*	100 ± 7	4.0 ± 0.8	1228 ± 57	0.077 ± 0.007	0.00573 ± 0.00023
Lodran silicate-rich 1200 °C*	12.7 ± 2.4	2.68 ± 0.19	88.9 ± 1.6	0.123 ± 0.027	0.0300 ± 0.0004
Lodran silicate-rich 1400 °C	58 ± 4	5.06 ± 0.06	5.07 ± 0.07	11.3 ± 0.8	0.13 ± 0.03
Lodran silicate-rich 1600 °C	23.8 ± 2.8	4.19 ± 0.14	11.35 ± 0.16	2.02 ± 0.25	0.121 ± 0.006
GRA 95209 Fe/Ni-rich 1000 °C*	433 ± 29	2.17 ± 0.18	4193 ± 106	0.082 ± 0.007	0.0321 ± 0.0004
GRA 95209 Fe/Ni-rich 1200 °C*	104 ± 7	1.20 ± 0.10	869 ± 28	0.062 ± 0.009	0.0882 ± 0.0005
GRA 95209 Fe/Ni-rich 1400 °C	50 ± 4	1.45 ± 0.06	184 ± 4	0.170 ± 0.021	0.1548 ± 0.0011
GRA 95209 Fe/Ni-rich 1600 °C	14.2 ± 2.2	1.61 ± 0.04	41.3 ± 0.5	0.23 ± 0.05	0.1693 ± 0.0013

*Blank correction >8% of the measured ^{36}Ar.
†Uncertainty probably accidentally low, given the ^{38}Ar amount of only 1×10^{-11} cm^3 measured with the Faraday cup.
‡When not given: release temperature = 1700 °C.
Abbreviations: GRA = Graves Nunataks; b.d. = below detection limit or uncertainty exceeding 100%.

Shallowater and Mount Egerton. Tatahouine, Lodran and GRA 952029 are less effected: using the Ba and rare earth element (REE) abundances given in Table A6, production rates by Eugster and Michel (1995), Hohenberg *et al.* (1981), and Shukolyukov and Begemann (1996a), and a cosmic-ray exposure age of 20 ± 2 Ma (Eugster and Michel, 1995), we can estimate the Xe_{cosm} abundance in Tatahouine. We obtain $^{126}Xe_{cosm} \approx (2 \pm 1) \times 10^{-15}$ cm^3/g and $^{130}Xe_{cosm} \approx (1.6 \pm 0.3) \times 10^{-15}$ cm^3/g in Tatahouine, which is 4–34% and 0.1–0.9% of the totally measured ^{126}Xe and ^{130}Xe concentrations, respectively. These values cannot be used to subtract Xe_{cosm}, because the Xe_{cosm} distribution in the temperature steps is unknown. Therefore, we determined Xe_{cosm} in Tatahouine, as for all other samples, *via* a two-component decomposition that is described below. The $^{124}Xe/^{130}Xe$ and $^{126}Xe/^{130}Xe$ ratios for Tatahouine (not shown) are identical to air, except for steps "Ta pow 8" and "Ta pow 17" (see Table 2). Accordingly, except for the latter two steps, no other Xe abundances in Tatahouine were corrected for Xe_{cosm}. For all measurements, $^{129-136}Xe_{cosm}$ contributions are negligible. The $^{124}Xe/^{130}Xe$ and $^{126}Xe/^{130}Xe$ ratios of Lodran, except for those of "Lo Si 16", indicate within errors pure trapped components, in agreement with the large trapped gas concentrations in Lodran and the cosmic-ray exposure age of 7.7 ± 1.2 Ma (Weigel *et al.*, 1999). Less than

TABLE 5. Kr concentrations and isotopic composition in bulk achondrites and mineral-rich separates of Lodran and Graves Nunataks 95209.

	^{86}Kr (10^{-12} cm^3/g)	$^{78}Kr/^{86}Kr$	$^{80}Kr/^{86}Kr$	$^{82}Kr/^{86}Kr$	$^{83}Kr/^{86}Kr$	$^{84}Kr/^{86}Kr$	$^{84}Kr_{tr}$ (10^{-12} cm^3/g)	$^{83}Kr_{cosm}$ (10^{-12} cm^3/g)
Tatahouine 800 °C	0.57 ± 0.09	2.2 ± 0.4	13.5 ± 1.0	62 ± 3	62 ± 4	322 ± 18	1.84 ± 0.10	b.d.
Tatahouine 1400 °C	0.93 ± 0.14	2.01 ± 0.06	12.2 ± 0.5	63.4 ± 2.3	63.6 ± 2.2	311 ± 10	2.89 ± 0.09	b.d.
Tatahouine	0.78 ± 0.12	3.03 ± 0.09	15.1 ± 0.8	68.5 ± 2.6	70.5 ± 2.7	326 ± 12	2.50 ± 0.10	0.038 ± 0.003
Tatahouine chunks 800 °C	0.81 ± 0.12	1.95 ± 0.06	13.7 ± 0.4	67.7 ± 1.5	65.8 ± 1.8	327 ± 8	2.63 ± 0.06	b.d.
Tatahouine chunks 1400 °C	10.7 ± 1.6	2.01 ± 0.06	12.7 ± 0.3	65.6 ± 1.7	66.3 ± 1.7	330 ± 8	35.1 ± 0.9	0.07 ± 0.04
Tatahouine chunks	4.3 ± 0.7	2.08 ± 0.12	13.5 ± 0.5	64.8 ± 1.4	65.2 ± 1.8	329 ± 8	14.3 ± 0.3	b.d.
Tatahouine powder 800 °C*	0.193 ± 0.029	2.05 ± 0.17	14.8 ± 1.0	67 ± 4	62 ± 3	323 ± 16	0.62 ± 0.03	b.d.
Tatahouine powder 1400 °C*	1.44 ± 0.27	2.0 ± 0.4	12.7 ± 2.4	65 ± 12	63 ± 12	307 ± 60	4.4 ± 0.9	b.d.
Tatahouine powder*	0.33 ± 0.05	3.65 ± 0.29	18.5 ± 1.7	73 ± 8	72 ± 8	306 ± 40	1.00 ± 0.13	0.0218 ± 0.0014
Norton County I	18.9 ± 2.8	4.57 ± 0.18	25.4 ± 0.7	82 ± 3	86 ± 3	343 ± 15	61.8 ± 2.8	3.873 ± 0.019
Norton County II	8.5 ± 1.3	6.48 ± 0.13	30.0 ± 0.8	90 ± 3	98 ± 3	350 ± 16	27.7 ± 1.4	2.718 ± 0.014
Cumberland Falls	20 ± 3	3.62 ± 0.13	94.0 ± 1.2	100.3 ± 2.6	74.8 ± 2.7	324 ± 13	63.7 ± 2.6	1.938 ± 0.010
Mount Egerton	26 ± 4	2.10 ± 0.06	13.6 ± 0.4	65.7 ± 1.7	65.1 ± 1.9	323 ± 9	84.3 ± 2.2	b.d.
Mayo Belwa1600 °C	26 ± 4	3.86 ± 0.09	26.8 ± 0.5	79.1 ± 1.5	80.1 ± 1.5	340 ± 7	86.0 ± 1.8	3.82 ± 0.12
Shallowater1600 °C	308 ± 46	2.039 ± 0.022	16.62 ± 0.19	67.7 ± 0.6	65.9 ± 0.6	325 ± 3	1001 ± 9	2.157 ± 0.011
Pasamonte*,†,‡	0.0 ± 2.2	69172 ± 3938	211137 ± 21540	351742 ± 103189	459206 ± 104170	294763 ± 509300	b.d.	5.569 ± 0.028
Lodran BE-551 Fe/Ni-rich-rich	1008 ± 151	1.85 ± 0.07	12.4 ± 0.3	64.9 ± 0.9	63.1 ± 0.9	314 ± 4	3164 ± 39	b.d.
Lodran Fe/Ni-rich-rich	497 ± 93	1.86 ± 0.17	12.1 ± 0.4	66.5 ± 1.5	65.7 ± 1.8	326 ± 8	1621 ± 39	b.d.
Lodran Fe/Ni-rich 2.5 h HF*	133 ± 20	2.9 ± 1.7	21 ± 9	81 ± 43	76 ± 43	358 ± 215	468 ± 285	13.7 ± 0.6
Lodran Fe/Ni-rich 1000 °C*	6.8 ± 1.2	3.5 ± 0.6	17.3 ± 1.9	77 ± 8	79 ± 9	352 ± 38	23.3 ± 2.6	0.90 ± 0.03
Lodran Fe/Ni-rich 1200 °C	23 ± 3	2.13 ± 0.12	12.8 ± 0.4	64.0 ± 1.8	65.1 ± 1.9	323 ± 9	74.3 ± 2.1	b.d.
Lodran Fe/Ni-rich 1400 °C	446 ± 67	1.999 ± 0.029	12.78 ± 0.13	65.9 ± 0.6	65.0 ± 0.5	320.6 ± 2.6	1431 ± 11	b.d.
Lodran Fe/Ni-rich 1600 °C*	8.9 ± 1.3	3.1 ± 0.6	13.08 ± 1.25	64 ± 5	67 ± 5	332 ± 23	29.4 ± 2.0	0.08 ± 0.03
Lodran Fe/Ni-rich 10 min HF	486 ± 73	2.00 ± 0.09	13.8 ± 0.4	69.5 ± 1.9	70.1 ± 1.9	337 ± 9	1625 ± 45	22.0 ± 2.0
Lodran troilite-rich	550 ± 83	1.98 ± 0.05	12.29 ± 0.28	64.1 ± 1.3	64.2 ± 1.3	318 ± 6	1751 ± 33	b.d.
Lodran Fe/Ni-rich 40 min HF	545 ± 82	1.92 ± 0.05	12.3 ± 0.3	64.5 ± 1.5	63.7 ± 1.6	315 ± 7	1719 ± 40	b.d.
Lodran silicate-rich 1000 °C	12.8 ± 1.9	2.37 ± 0.17	12.1 ± 0.9	72 ± 4	67 ± 4	312 ± 20	39.8 ± 2.5	0.23 ± 0.05
Lodran silicate-rich 1200 °C*	7.0 ± 1.1	2.4 ± 0.3	14.3 ± 1.4	68 ± 7	66 ± 6	322 ± 32	22.6 ± 2.2	0.057 ± 0.027
Lodran silicate-rich 1400 °C	334 ± 50	2.07 ± 0.07	14.1 ± 0.7	69.2 ± 2.3	69.6 ± 2.6	344 ± 15	1141 ± 49	13.5 ± 1.3
Lodran silicate-rich 1600 °C	53 ± 8	1.98 ± 0.05	12.8 ± 0.3	64.0 ± 1.2	62.5 ± 1.2	311 ± 6	164 ± 3	b.d.
GRA 95209 Fe/Ni-rich 1000 °C	32 ± 5	2.20 ± 0.07	13.4 ± 0.3	66.9 ± 1.5	67.3 ± 1.5	323 ± 7	103.0 ± 2.4	0.56 ± 0.12
GRA 95209 Fe/Ni-rich 1200 °C	12.7 ± 1.9	2.44 ± 0.13	13.7 ± 0.8	64 ± 3	61 ± 3	308 ± 16	39.0 ± 2.0	b.d.
GRA 95209 Fe/Ni-rich 1400 °C*	6.6 ± 1.0	2.58 ± 0.24	16.1 ± 1.4	72 ± 7	69 ± 7	330 ± 32	21.6 ± 2.1	0.227 ± 0.026
GRA 95209 Fe/Ni-rich 1600 °C*	6.4 ± 1.0	1.9 ± 0.3	13.9 ± 1.7	69 ± 8	69 ± 8	326 ± 38	20.8 ± 2.4	0.186 ± 0.025

Isotopic ratios normalised to $^{86}Kr = 100$.
*Blank correction >20% of the measured ^{86}Kr.
†Pasamonte: $^{81}Kr/^{86}Kr = 13455 \pm 1106$.
‡Large uncertainties due to ~100% blank correction of reference isotope ^{86}Kr.
Abbreviations: GRA = Graves Nunataks; b.d. = below detection limit.

~1% of the ^{126}Xe and 0.1% of the ^{130}Xe in bulk Lodran are cosmogenic and thus only "Lo Si 16" has been corrected (Table 3). Similarly, in the *Fe/Ni*-rich GRA 95209 separate, at maximum 15% of the measured ^{126}Xe and 0.4% of the ^{130}Xe can be cosmogenic, if we conservatively adopt the estimate for the *silicate*-rich bulk sample with an exposure age of 6.8 ± 0.6 Ma (Terribilini *et al.*, 2000). Xe_{cosm} in the 1200 and 1600 °C was subtracted, the other two steps were not corrected (Table 3).

In general, cosmogenic Xe was subtracted using the $^{126}Xe_{cosm}$ concentrations (Tables 3 and A3) and Xe_{cosm} spectra (Table A5). The latter are determined as follows: the main target elements for the production of Xe_{cosm} are Ba and the REE La, Ce and Nd. We calculated the Xe_{cosm} composition for the different bulk samples with spectra given by Hohenberg *et al.* (1981) obtained from Angra dos Reis, depending on the Ba and REE concentrations (Table A6). The compositions of Xe_{cosm} produced from Ba and the REEs, respectively, are significantly distinct (Fig. 1). The resulting cosmogenic compositions (Table A5) are schematically shown in Fig. 1. Another approach to obtain Xe_{cosm} spectra is to use model calculations based on irradiation experiments of artificial meteoroids (*e.g.*, Leya *et al.*, 2000 and references therein). However, such experiments yielded so far only isotopic ratios for Xe produced from Ba by irradiation with a monoenergetic proton beam (Mathew *et al.*, 1994). Thus, the resulting Xe isotopic ratios (Table A5) do not represent the complex irradiation conditions in space, nor take into account the Xe production in REE (Table A5).

The concentrations of $^{126}Xe_{cosm}$ (Tables 3 and A3) were separately determined *via* the $^{128}Xe/^{126}Xe$ and $^{130}Xe/^{126}Xe$ ratios. Concentrations obtained with both methods agree within 5% for all samples with significant Xe_{cosm} concentrations. Cumberland Falls shows a neutron-induced excess of ^{128}Xe (see also Fig. 9 and Lorenzetti *et al.*, 2002). Therefore, we

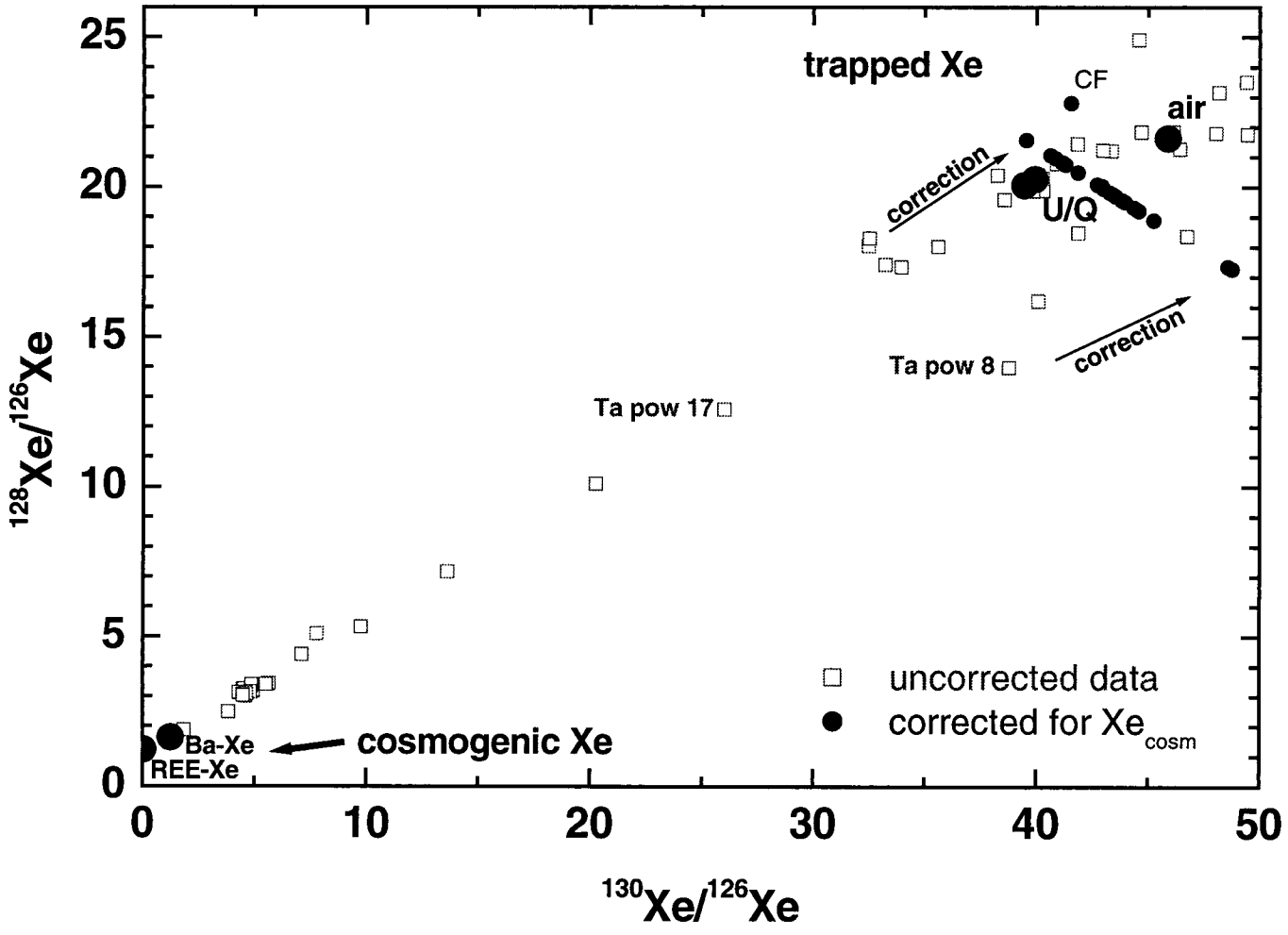

FIG. 1. Schematically shows the correction for Xe_{cosm}. Decomposition of the measured abundances was performed using separately both the $^{128}Xe/^{126}Xe$ and $^{130}Xe/^{126}Xe$ ratios. The cosmogenic endmember compositions (Table A5) are based on spectra given by Hohenberg *et al.* (1981) and the target element concentrations as listed in Table A6. We determined $^{126}Xe_{cosm}$ for each possible trapped component U-Xe, air and Xe-Q separately. The $^{126}Xe_{cosm}$ concentrations in Tables 6 and A3 are averages of all six possibilities. Samples that plot around air were not corrected. Cumberland Falls was corrected using the $^{130}Xe/^{126}Xe$ alone due to n-induced excess of ^{128}Xe.

used the $^{130}Xe/^{126}Xe$ ratio only. Figure 1 shows the bulk data obtained in this work. All measured data points plot between the cosmogenic and trapped endmembers. The trapped Xe composition is *a priori* unknown. We calculated $^{126}Xe_{cosm}$ separately for the three possible candidates air, Xe-Q and U-Xe as endmembers with $^{128}Xe/^{126}Xe = 21.62/20.27/20.06$ and $^{130}Xe/^{126}Xe = 45.87/39.92/39.46$ for air/Xe-Q/U-Xe, respectively. The $^{126}Xe_{cosm}$ concentrations given in this manuscript are averages of the values obtained for both Xe isotopic ratios and the three trapped components. The uncertainties cover each of these six possibilities. The resulting $^{132}Xe_{tr}$ concentrations are given in Tables 3 and A3. The corrections for Xe_{cosm} amount to up to 98% of the measured ^{126}Xe but to <4% of the measured ^{132}Xe.

We do not correct the Xe *isotopic* composition for Xe_{fiss}, because fissiogenic contributions have been included in the analysis by Pepin and Phinney (1978) and Takaoka (1972). The spread of the Xe isotope data due to fissiogenic contributions allows extrapolating mixing lines for achondrites towards the trapped composition (see below). Here, Pasamonte and D'Orbigny, and to a lesser extent Sahara 99555 and Millbillillie, show significant Xe_{fiss} concentrations (Tables 3 and A3). For the discussion of the *element* abundances we subtract from the spallation-corrected data the $^{132}Xe_{fiss}$ concentrations with $(^{132}Xe/^{130}Xe)_{tr} = 6.33 \pm 0.28$. The large uncertainty includes all three possible trapped Xe components. The contribution of $^{84}Kr_{fiss}$ in all samples is <0.03% (0.5% for D'Orbigny) of the non-cosmogenic ^{84}Kr and thus negligible. We used $(^{86}Kr/^{136}Xe)_{fiss} = 0.019 \pm 0.005$ (Lewis, 1975).

DISCUSSION OF THE NEW XENON DATA

Figures 2–6 show the Xe isotopic composition of the samples analysed in this work corrected for Xe_{cosm}, where necessary (Tables 3 and A3). Included are the data points for air, Q and U (see Table 1 for references). Our new data scatter

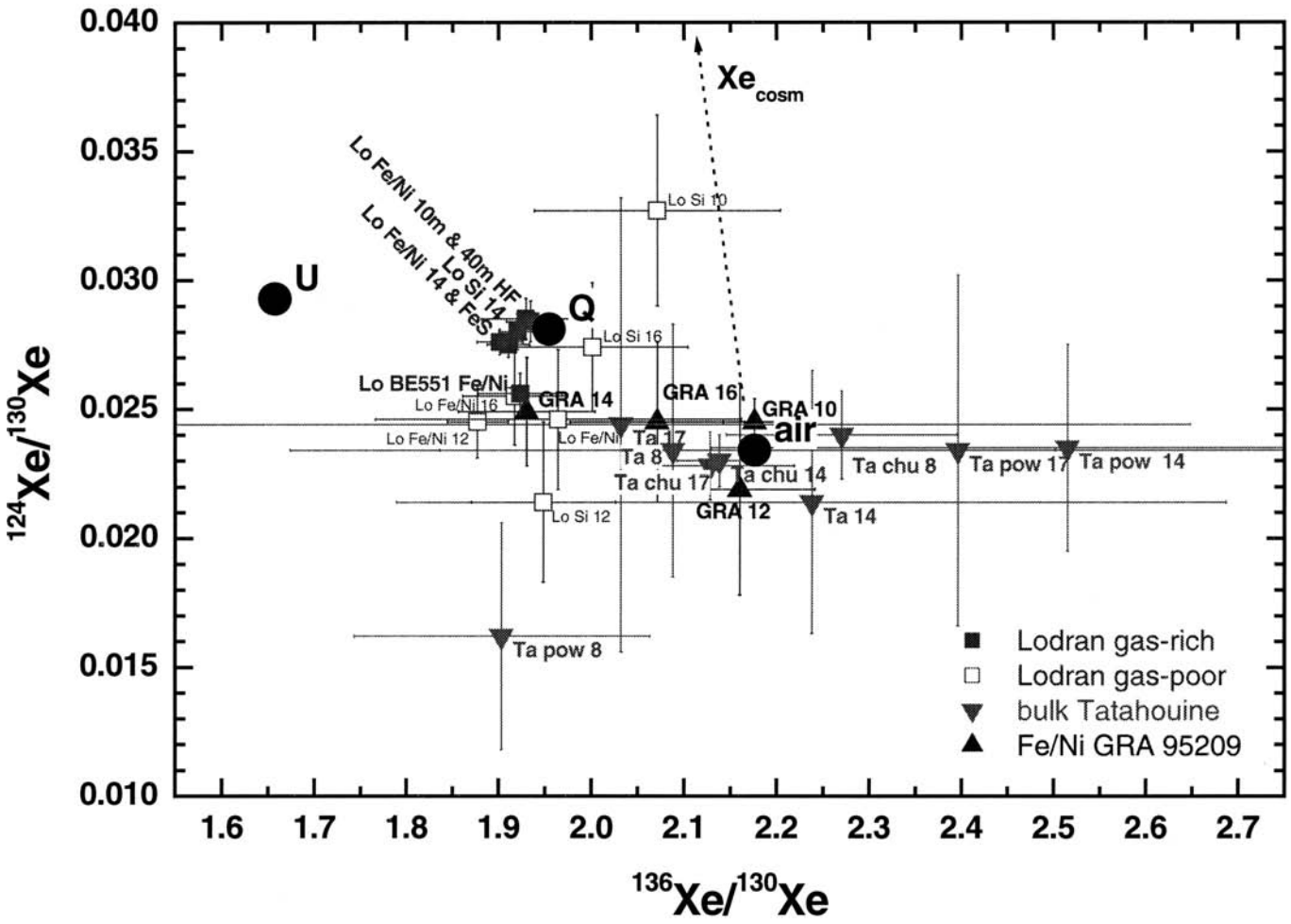

FIG. 2. $^{124}Xe/^{130}Xe$ and $^{136}Xe/^{130}Xe$ ratios as measured in Tatahouine and the separates of Lodran and GRA 95209. All Xe isotopic ratios are consistent with mixtures of Xe-Q and absorbed terrestrial Xe. The gas-rich measurements of Lodran contain almost pure Xe-Q. The significant gap between the measured data field and U-Xe composition suggests an endmember composition of the originally trapped Xe close to Xe-Q. Only "Ta pow 8", "Ta pow 17", "Lo Si 16", "GRA 12" and "GRA 16" were corrected for Xe_{cosm} (see Table 3). Abbreviations are given in Table 2.

around the data points for Q and air. The data for the whole-rock samples as well as the separates are not consistent with U-Xe as the trapped component for all isotopic ratios. In particular, there is a significant gap between U-Xe and the data fields measured in this work, which suggests a discrete trapped Xe endmember composition close to Xe-Q rather than a mixture of U-Xe with other components. The main, gas-rich steps of Lodran (Figs. 2 and 3; see also Tables 1 and 3) indicate Q composition. The less gas-rich measurements scatter around Q and air composition due to some terrestrial contamination and large statistical uncertainties. The sample set includes an aliquot of "BE-551 Fe/Ni", one of the metal-rich separates of Lodran identified by Weigel and Eugster (1994) as U-Xe-bearing. Surprisingly, our analysis reveals the presence of Xe-Q rather than U-Xe. The Xe isotope patterns of the six most gas-rich Lodran steps (^{132}Xe concentrations $>8 \times 10^{-10}$ cm^3/g; Table 3) and their average are plotted in Fig. 4, normalised to Xe-Q (Busemann *et al.*, 2000). All isotope ratios point to Q composition. In Table 1, we give the average of the main Lodran measurements with standard deviation. The trapped Xe in all our samples of Lodran turns out to be—within 2σ—Xe-Q. The small discrepancy between Xe-Q and the Lodran average in ^{134}Xe and ^{136}Xe might indicate some modification of Xe-Q, which was determined mainly in carbonaceous chondrites, due to some contamination with Xe-HL from presolar diamonds.

Lodran is an especially gas-rich achondrite with Xe concentrations almost reaching those in carbonaceous chondrites. Surprisingly, the metal- and troilite-rich separates contain high concentrations of trapped Xe, exceeding those found in silicate-rich separates or bulk measurements (Kim *et al.*, 1995; Weigel, 1996; Zähringer, 1968). The unambiguous identification of the probably secondary gas-bearing phase failed. Kim *et al.* (1995) suggested gas bubbles associated with silicate inclusions within the metal. Here, we do not discuss the gas-rich minerals in detail, because we cannot exclude that the handpicked separates contain minor inclusions or intergrown minerals of other material. However, we emphasize that all

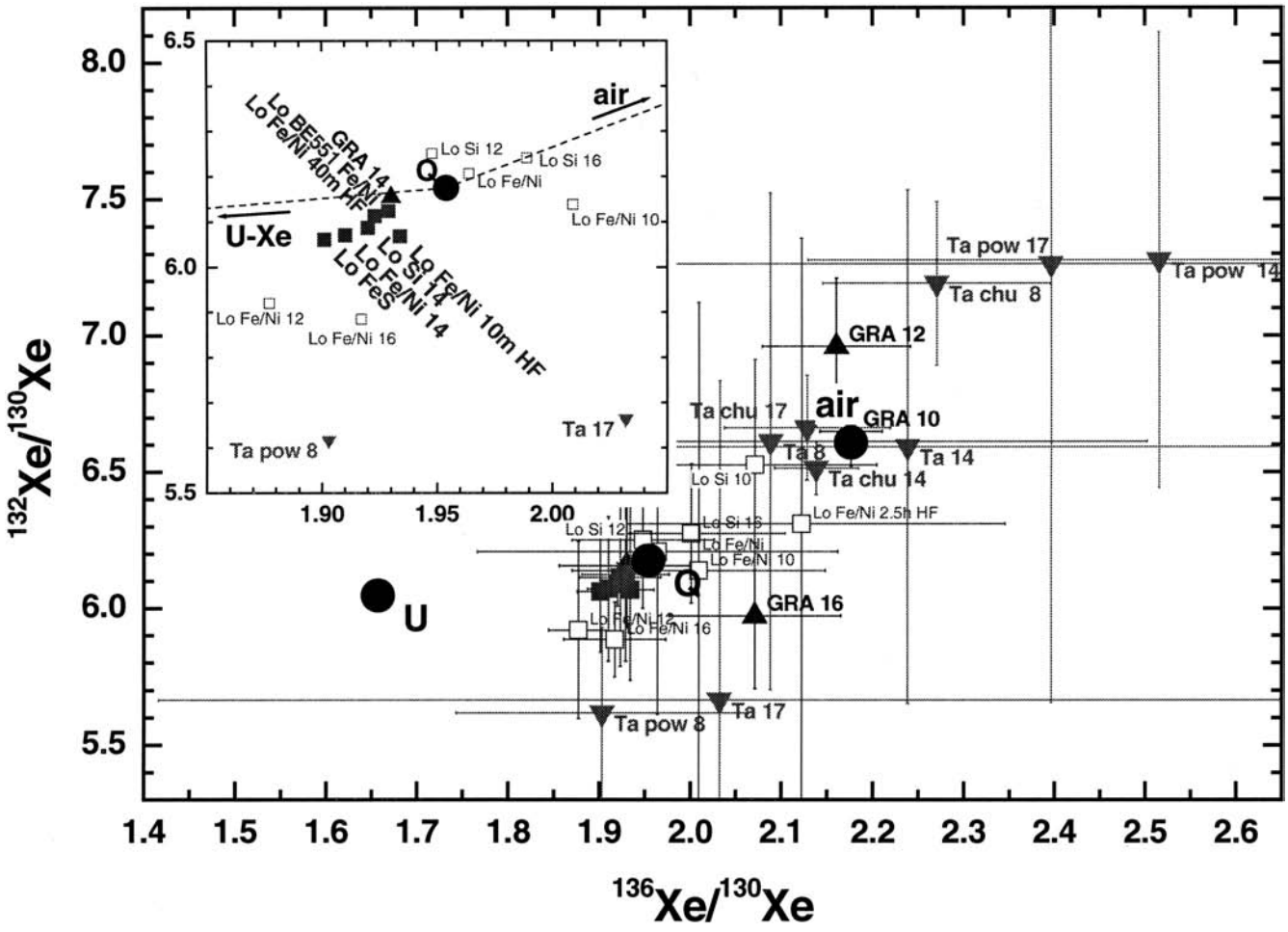

FIG. 3. ^{132}Xe/^{130}Xe and ^{136}Xe/^{130}Xe ratios in Tatahouine, Lodran and GRA 95209. All data suggest Xe-Q and terrestrial Xe rather than U-Xe composition. See Fig. 2 for legend and labels.

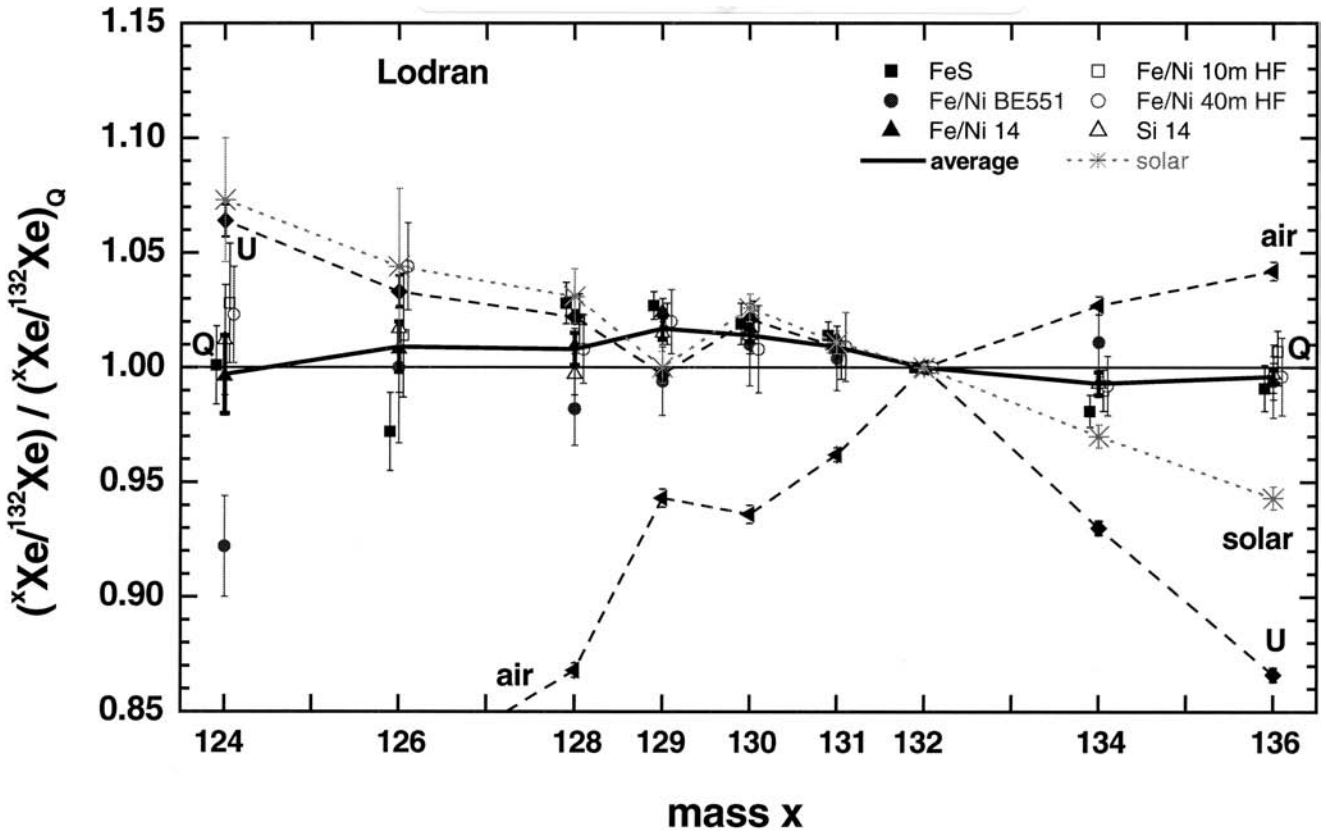

FIG. 4. Xenon isotopic patterns of the six most gas-rich Lodran measurements and their average (see also Tables 1 and 3), U-Xe (Pepin, 2000), air and solar Xe. All data are normalised to Xe-Q composition (Busemann *et al.*, 2000). The average (listed in Table 1) agrees with Xe-Q composition within 2σ uncertainty. Cosmogenic Xe is negligible in all six measurements. Solar composition from Pepin *et al.* (1995).

separates (silicate-rich, FeS-rich, metal-rich) contain within a factor of 3 comparably large amounts of trapped Xe (Table 3), indicating that the host of the trapped noble gases is widespread and not exclusively related to a certain separate. This is supported by the identical main gas release temperature of 1400 °C for the metal-rich and silicate-rich separates.

Rather speculatively we suggest that the matrix-related carbonaceous carrier phase Q that originally was distributed within the pre-metamorphic chondritic parent-body, preferentially accumulated during metamorphism in the liquid metal phase and thus led to an enrichment of the noble gases in the metallic phases (see Vogel *et al.*, 2002, for a comparable mechanism during chondrule melting).

The Tatahouine samples contain only small amounts of trapped Xe (Table 3) and even the major steps contain Xe that is close to air in composition (Figs. 2 and 3). Different pieces of Tatahouine (Table 2) were measured to verify our first results (Busemann and Eugster, 2000a). We measured samples crushed to powder, as a set of chunks and in a single piece to test possible air contamination due to preparation in the laboratory. Unexpectedly, the powder contains 1 order of magnitude less (atmospheric) Xe than the less fine-grained samples, suggesting that the terrestrial contamination has been introduced prior to the sample preparation. Achondrites in general have proven to trap significant amounts of air during weathering processes (*e.g.*, Gilmour *et al.*, 2001; Niedermann and Eugster, 1992; Shukolyukov and Begemann, 1996b). Barrat *et al.* (1998) demonstrated the effects of 63 years of terrestrial weathering on Tatahouine. The Tatahouine sample measured by Michel and Eugster (1994) indicated U-Xe composition in the 1000 and 1200 °C steps containing ~30% of the totally released gas ($^{132}Xe_{total} = (11–14) \times 10^{-12}$ cm^3/g). The Tatahouine chunks contain a similar amount of terrestrial Xe ($^{132}Xe_{total} = 16 \times 10^{-12}$ cm^3/g), while the other two samples contain only ~2 × 10^{-12} cm^3/g of ^{132}Xe (see Table 6 for a comparison with other diogenites).

The metal-rich separate of GRA 95209 (Figs. 2, 3 and 5) was measured in similar steps as Lodran to test whether the large concentration of Xe-Q in Lodran is typical for lodranites in general. Excluding the 1000 °C step, which clearly contains pure air (Fig. 5), the Xe concentration is ~10 to 40× smaller than those in comparable Lodran separates (Table 3). A silicate-rich separate of GRA 95209 was measured by Terribilini *et al.* (2000). The total ^{132}Xe concentration of 180 × 10^{-12} cm^3/g in

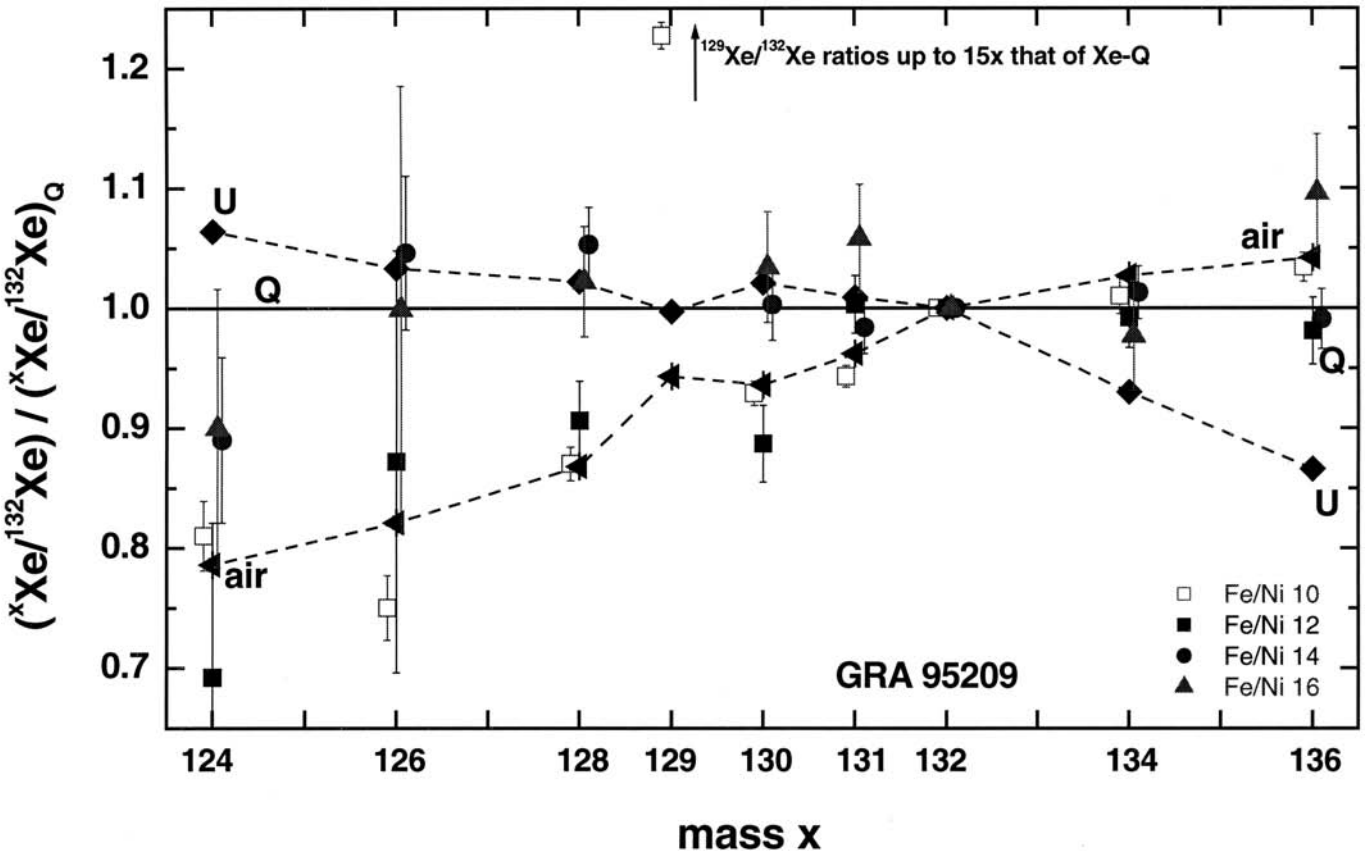

FIG. 5. The Xe isotopic composition of the metal-rich separate of GRA 95209 lodranite in a plot similar to Fig. 4. GRA 952029 metal shows mainly terrestrial Xe composition. The 1400 °C step contains Xe-Q. Abbreviations are given in Table 2, references in Fig. 4.

the silicates (Table 6) is much lower than that found here for Lodran but 3× larger than that measured in our GRA 95209 metal-rich separate (without the 1000 °C step). This indicates that the enrichment of the trapped Xe in bulk Lodran and especially in the non-silicate phases is not a general feature of lodranites but can be attributed to certain conditions during the formation of the metals of Lodran solely. The composition of the 1400 °C step of the GRA 95209 metal-rich sample suggests roughly Q composition within the rather large uncertainties (Fig. 5), in agreement with the more precise data of the silicate-rich separate (Terribilini *et al.*, 2000) that contains pure Xe-Q.

The metal-rich sample of GRA 95209 contains large excesses of radiogenic ^{129}Xe leading to a high $^{129}Xe/^{132}Xe$ ratio of 15.5 in the 1200 °C step compared to only 6.0 in the silicate-rich phase (Terribilini *et al.*, 2000), whereas the $^{132}Xe_{tr}$ concentrations in both separates are comparable. The excess might allow dating the formation of the metal grains, assuming that they consist of a single mineral phase. We therefore performed a first analysis of some neutron-irradiated grains of this sample in order to determine the I-Xe systematics (Whitby *et al.*, 2002). However, the severe weathering experienced by this Antarctic meteorite led to almost completely rusty grains which appears to have resulted in contamination with both terrestrial Xe and I of the investigated samples (Whitby *et al.*, 2002).

The new Xe isotopic data for several other aubrites and angrites are shown in Fig. 6. Here, all data had to be corrected for Xe_{cosm}. The corrected data are consistent with mixtures of small amounts of trapped Xe-Q, air and significant amounts of fission Xe in Pasamonte, Sahara 99555, D'Orbigny, Millbillillie and Norton County (see Fig. 8 for the off-scale data points of Pasamonte and D'Orbigny). Again, the apparent gap between the data and U-Xe composition suggests an endmember composition close to Q. In particular, the data points for Norton County, which has been reported to contain U-Xe, are consistent with a mixture of Xe-Q or air and fission Xe. Shallowater and Cumberland Falls contain pure Xe-Q. This most likely reflects the distinct, non-brecciated origin of Shallowater from a different parent body than the other aubrites and the abundant chondritic fragments found in Cumberland Falls (Keil, 1989, and references therein). The $^{132}Xe_{tr}$ concentrations in Shallowater and Cumberland Falls as measured here are 10–50× higher than those in the other aubrites (Majo Belwa, Mt. Egerton, Norton County, and Peña Blanca Spring), which show mixtures of Xe-Q and air (Tables 3 and 6). The variation of the

TABLE 6. ^{132}Xe concentrations and Xe isotopic composition ($^{129}Xe/^{132}Xe$ excluded) in several bulk achondrites.

Sample	Class	^{132}Xe (10^{-12} cm^3/g)	Xe isotopic composition	Reference
Primitive achondrites				
Yamato-74357	Lodranite	53 ± 5	Air	Takaoka *et al.* (1993)
Yamato-74357	Lodranite	48 ± 5	Air	Nagao *et al.* (1995)
Graves Nunataks 95209 (silicates)	Lodranite	180 ± 51	Q	Terribilini *et al.* (2000)
Yamato-74063	Acapulcoite	66500 ± 6650	Q	Takaoka *et al.* (1993)
Monument Draw	Acapulcoite	1120 ± 80	Q	McCoy *et al.* (1996)
Acapulco	Acapulcoite	460 ± 80	–	Palme *et al.* (1981)
Mt. Morris	Winonaite	~1000	Q*	Garrison and Bogard (1997)
Winona	Winonaite	~300	Q + air*	Garrison and Bogard (1997)
Pontlyfni	Winonaite	~200	Air*	Garrison and Bogard (1997)
Divnoe	Ungrouped	108 ± 17	Q	Weigel *et al.* (1997)
Divnoe	Ungrouped	255/258 ± 25	~Q + solar wind	Shukolyukov *et al.* (1995)
Brachina	Brachinite	55.5 ± 22.5	Q	Ott *et al.* (1993), quoted in Weigel *et al.* (1997)
Allan Hills 84025	Brachinite	35.4 ± 0.9	–	Ott *et al.* (1993)
Eagle Nest	Brachinite	38/58	Air	Swindle *et al.* (1998)
Lewis Cliff 88763	Brachinite	238	Q	Swindle *et al.* (1998)
Achondrites				
Cumberland Falls	Aubrite	3	–	Miura *et al.* (1999)
Majo Belwa	Aubrite	9	Air	Miura *et al.* (1999)
Mt. Egerton	Aubrite	33	Air	Miura *et al.* (1999)
Norton County	Aubrite	5	Air	Miura *et al.* (1999)
Peña Blanca Spring	Aubrite	4	Air	Miura *et al.* (1999)
Kapoeta	Howardite	360†	Q	Becker *et al.* (1998)
Petersburg	Howardite	13.7	Air assumed	Shukolyukov and Begemann (1996b)
15 eucrites	Eucrite	7–517	Air assumed	Shukolyukov and Begemann (1996b)
9 Yamato eucrites	Eucrite	11–53	Air assumed	Miura *et al.* (1993)
4 diogenites	Diogenite	5–28	Air	Michel and Eugster (1994)
Tatahouine	Diogenite	12.7 ± 2.0	Air + U	Michel and Eugster (1994)
Asuka 881371	Angrite	37 ± 21	–	Weigel *et al.* (1997)
Lewis Cliff 86010	Angrite	31 ± 20	Air assumed	Eugster *et al.* (1991)
Lewis Cliff 86010	Angrite	18.9	–	Hohenberg *et al.* (1991)
Angra dos Reis	Angrite	22.2	–	Hohenberg (1970)

*Garrison and Bogard compared the winonaites' Xe isotopic composition with AVCC-Xe, which consists of Xe-Q and Xe-HL, and concluded that Mt. Morris indicates solar Xe. A comparison with Xe-Q reveals however that Mt. Morris contains pure Xe-Q and the other winonaites a mixture of Xe-Q and air (or Xe-HL).
†Includes possibly some solar wind Xe, sample contains solar wind He-Ar.

$^{132}Xe_{tr}$ concentrations by a factor of ~40 in Cumberland Falls (Tables 3 and 6) might be the result of varying abundances of chondritic material in this aubrite.

The reason for the differing observations for Tatahouine and Lodran in this and previous work remains unclear. A too "pessimistic" overestimated blank correction would shift a possibly present Q composition towards U. This is demonstrated in Fig. 7 which shows the Lodran separate data given by Weigel (1996). We overcorrected a hypothetical mixture composed of 95% Xe-Q and 5% air (referred to ^{132}Xe) with 10–50% contributions of air. The results are given in the figure, labelled with "Q-10%" and so on. In fact, the Lodran data follow a trend towards a composition in linear extrapolation of the Q–air mixing line rather than towards U-Xe (Fig. 7). Some data even plot beyond the composition of U-Xe. However, the absolute ^{132}Xe amounts measured in these samples, given as numbers (in 10^{-12} cm^3) close to the data points, do not univocally support this view. Large blank corrections of up to 50% of the measured ^{132}Xe, however, must have been applied to explain the variations.

THE ORIGINAL OBSERVATIONS OF U-XENON

In this section, we reevaluate the experimental evidence for U-Xe found by Takaoka (1972) and Pepin and Phinney (1978). We are going to conclude that all data presented by these authors can be explained as mixtures of Xe-Q, air and fission Xe and

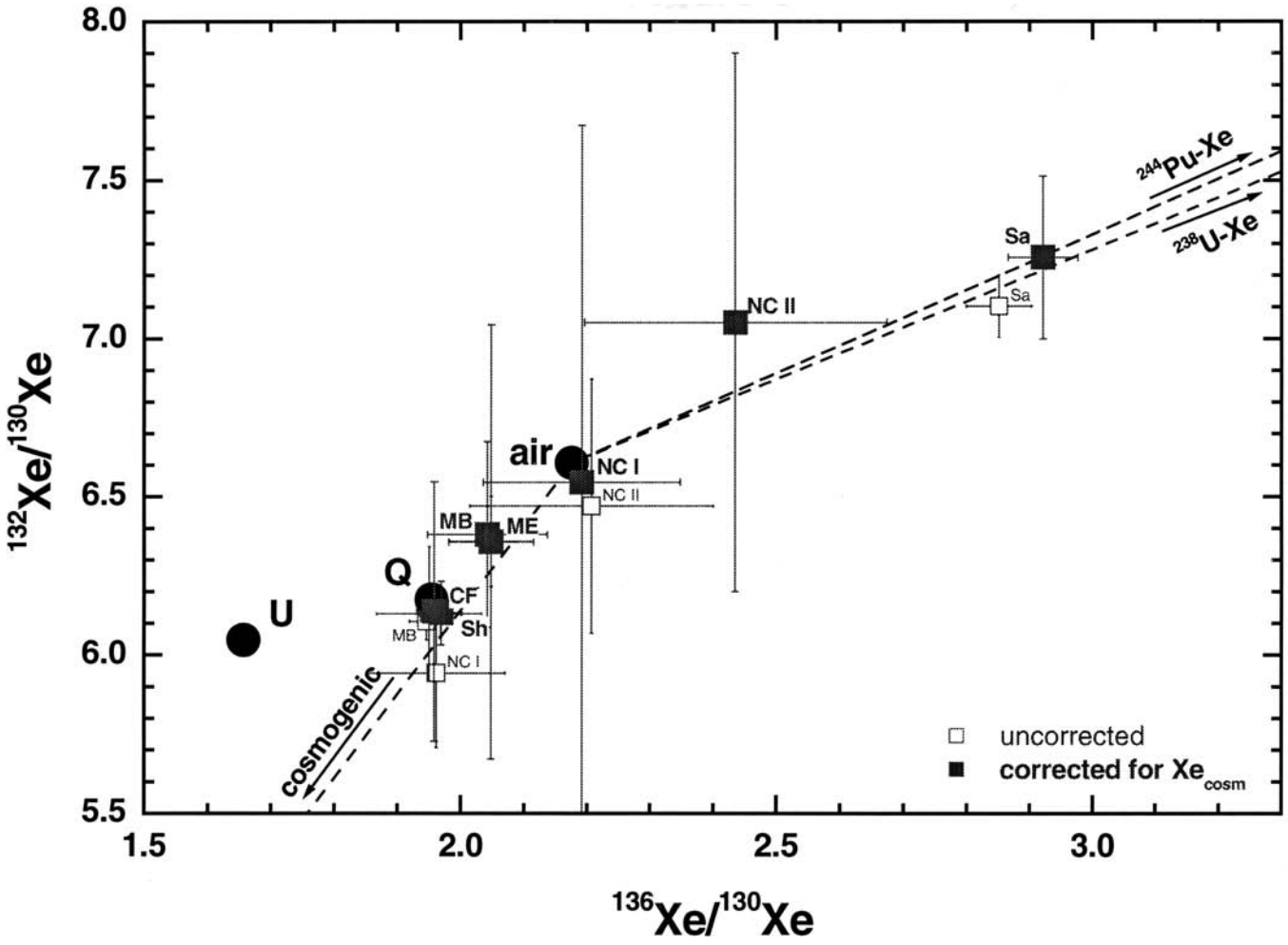

FIG. 6. $^{132}Xe/^{130}Xe$ *vs.* $^{136}Xe/^{130}Xe$ isotope plot showing the bulk aubrite and angrite measurements. The contributions of Xe_{cosm} were corrected for with the $^{128}Xe/^{126}Xe$ and $^{130}Xe/^{126}Xe$ ratios, except for Cumberland Falls that contains some ^{128}Xe-excess due to neutron capture. All data indicate mixtures of air and Xe-Q. D'Orbigny (not shown), Sahara 99555 and Norton County II contain various amounts of fission Xe (see also Fig. 8 for D'Orbigny). Cumberland Falls and Shallowater carry dominantly Xe-Q. Abbreviations are given in Table 2.

do not indicate the presence of U-Xe. However, due to lack of detailed information, we cannot give reasons for the discrepancies. Takaoka's original paper describes the extrapolation of achondritic and chondritic Xe isotopic data in three-isotope-plots towards a common *primitive* trapped composition. The achondrite data were corrected for Xe_{cosm} and form a mixing line including the fissiogenic Xe data point. The intersection of this line with a second mixing line finally determines U-Xe. The second, chondritic mixing line is based on chondritic data including "Xe-H", a component originating from presolar diamonds, solar wind Xe and common Xe-Q (see Fig. 8). At the time of publication of that work, the origin of Xe-H was not known. Now, the isotopic composition of this chondritic component is well determined (Huss and Lewis, 1994) and we included it in our plots.

Takaoka's correction for cosmogenic Xe has not been discussed in detail. We use the original data (Pasamonte: Hohenberg *et al.*, 1967; Norton County: Munk, 1967) and correct them according to the procedure outlined above. Interestingly, Takaoka used data from the H5 chondrite Achilles (Rowe *et al.*, 1965) for the achondritic data fit. We do not include this data point in our analysis, because of Achilles' chondritic nature. Pepin and Phinney (1978) used the data sets from stepwise heating of Pasamonte (Hohenberg *et al.*, 1967) and Angra dos Reis (Hohenberg, 1970). They corrected the data for cosmogenic Xe according to the method of Hohenberg *et al.* (1967). This method includes the variation of cosmogenic Xe isotopic ratios until the fits of the corrected non-cosmogenic data points in Xe-three-isotope plots have reached best quality. Pepin and Phinney used the cosmogenic ratios given in Table A5 (fifth column), which significantly disagree from the other data sets for Pasamonte. According to the authors, after correction the data set pointed to U-Xe composition and therefore supported their theoretical determination of U-Xe. For

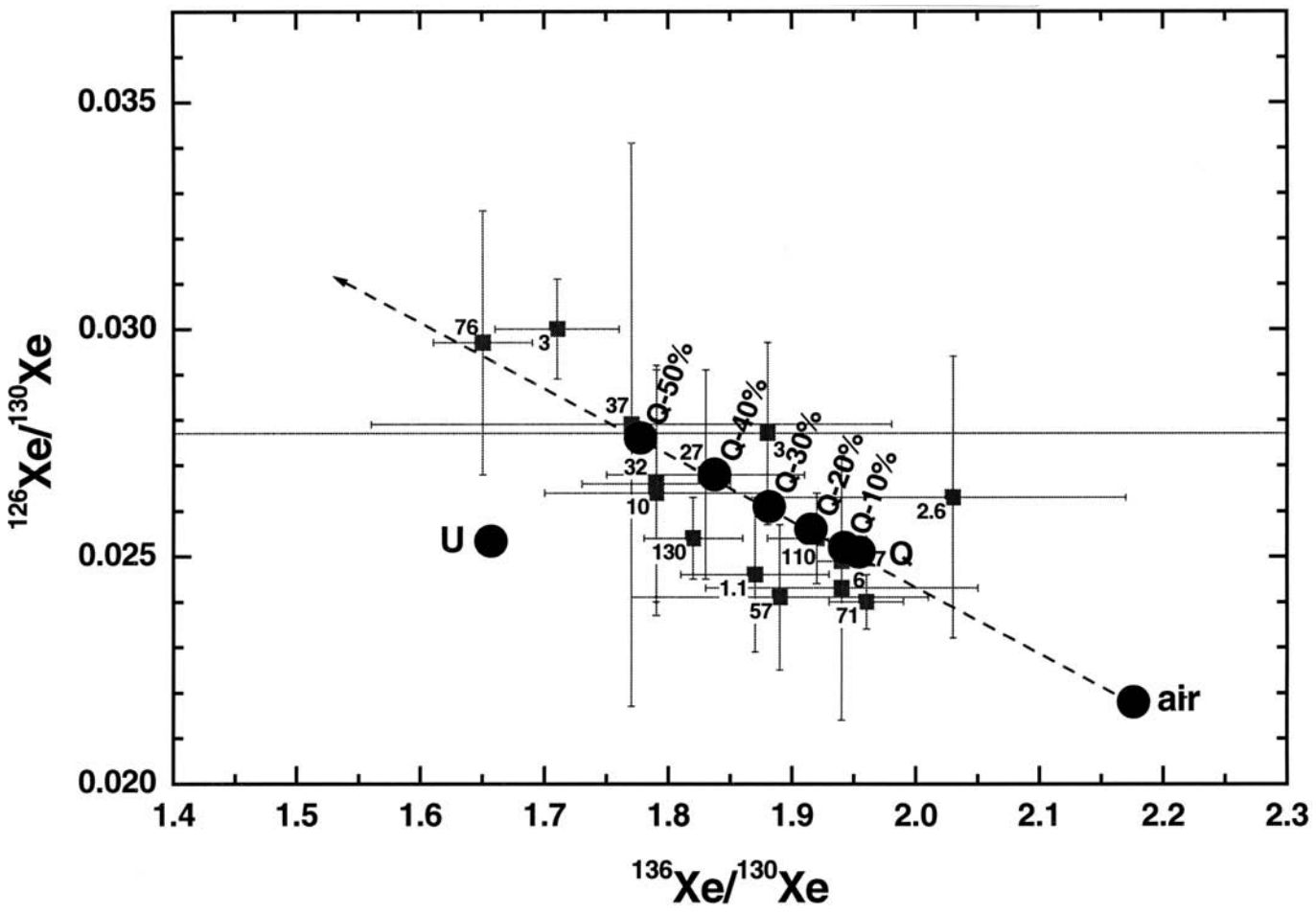

FIG. 7. The Xe isotopic data for Lodran metal as measured by Weigel (1996) plot close to the extrapolated mixing line of Q and air rather than indicate pure U-Xe composition. The data points labelled with "Q-xx%" represent a hypothetical mixture of 95% Xe-Q and 5% air, overcorrected with the subtraction of xx% blank of terrestrial Xe composition. The numbers represent the absolute amounts of ^{132}Xe in the respective samples in 10^{-12} cm^3 (Weigel, 1996). We excluded steps containing $<1 \times 10^{-12}$ cm^3 ^{132}Xe.

comparison, we visually read off the coordinates of their "achondrite correlation" line, shown in Fig. 8.

Here, we will use the spallation Xe systematics developed by Hohenberg *et al.* (1981) to correct for cosmogenic Xe (Table A5). These data were not available at the time of the determination of U-Xe. The newly corrected data for Pasamonte and Angra dos Reis again form a mixing line between fissiogenic Xe and a trapped component. However, our lines are slightly shifted relative to that defined by Pepin and Phinney (1978) (Fig. 8). All new fits are consistent with Xe-Q or air as the trapped component and do not point to U-Xe. Figure 8 shows the three lines fitting the data sets for Pasamonte, Angra dos Reis and the bulk data for Pasamonte taken from Shukolyukov and Begemann (1996b) and this work. The fits, though not forced through the fission Xe data points, almost perfectly hit this composition and thus indicate the reliability of the analyses. The reason for the discrepancies cannot simply be the different choice of the cosmogenic Xe spectra: starting with the same $^{126}Xe_{cosm}$ abundances as given in Table 3 and using Pepin and Phinney's $(^{132}Xe/^{126}Xe)_{cosm}$ ratio, the trapped $^{132}Xe/^{136}Xe$ ratios changes by <0.2%.

The inset of Fig. 8 shows the bulk data for the aubrites corrected for cosmogenic Xe as determined by Munk (1967), Rowe and Bogard (1966) and in this work. Unfortunately, the database of Xe measurements in these achondrites is rather small. The spread of the data is considerable and the U-Xe endmember composition of the trapped Xe cannot be excluded from this plot. However, we note that all data plot very close to Q or air and thus leave a large gap to U-Xe. This indicates that the trapped endmember composition is more likely to be close to Q.

U-XENON AND THE EVOLUTION OF THE ACHONDRITIC PARENT BODIES

The suggested presence of the most primitive U-Xe in achondrites and primitive achondrites of different classes,

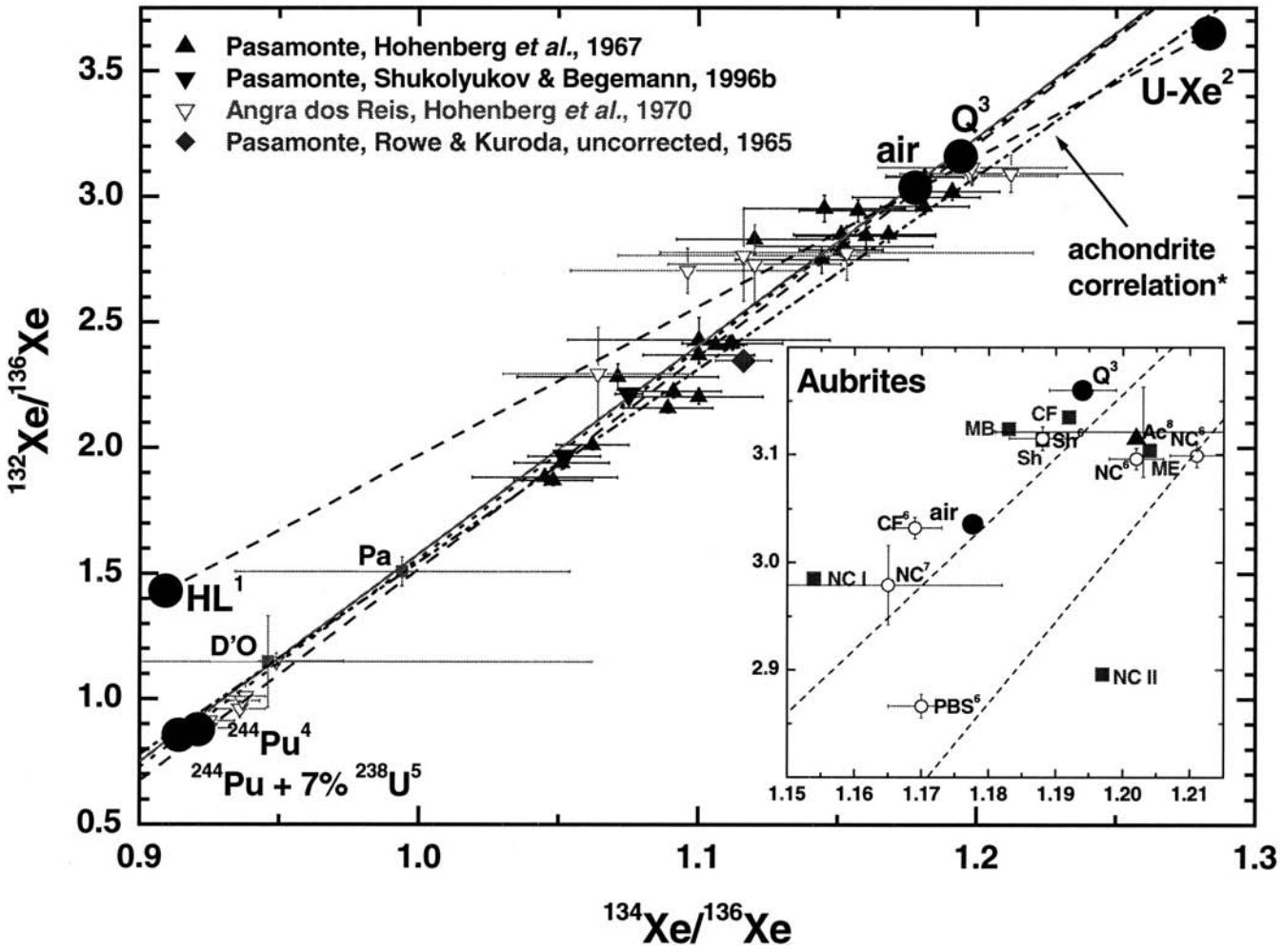

FIG. 8. The data for Pasamonte and Angra dos Reis can most straightforwardly be explained by binary mixtures of fission Xe and Xe-Q or air. No data point exceeds the Xe-Q data point towards a more primitive composition. All data were corrected for Xe_{cosm}. Fits through all three data sets (Angra dos Reis: Hohenberg (1970), Pasamonte: Hohenberg *et al.* (1967), and bulk Pasamonte: Shukolyukov and Begemann (1996b) and this work) suggest a mixture of Xe-Q and air on one side and fission Xe on the other. To the contrary, Pepin and Phinney (1978) obtained a correlation, based on the same data set, between U-Xe and fission Xe. We read out the coordinates of the mixing line (*) from the original figure. The large uncertainty of our data point for Pasamonte is due to a blank correction of 22% of the measured ^{132}Xe. The measurement of D'Orbigny was hampered by the release of large amounts of reactive gases. *Inset.* Bulk data for the aubrite Norton County and the H5 chondrite Achilles have been used to determine U-Xe composition (Takaoka, 1972). The new data for aubrites from this work and the data from literature do not exclude U-Xe composition within their large uncertainties (uncertainties for the new data comparable to size of inset). However, most data are more consistent with Q or air as trapped endmember composition and none of the data points indicates a more primitive composition than Xe-Q. See Table 2 for labels; PBS = Peña Blanca Spring, AC = Achilles. References: 1 = Huss and Lewis (1994); 2 = Pepin (2000); 3 = Busemann *et al.* (2000), 4 = Alexander *et al.* (1971), 5 = Eikenberg *et al.* (1993), 6 = Rowe and Bogard (1966), 7 = Munk (1967), 8 = Rowe *et al.* (1965). For comparison: uncorrected data point for Pasamonte from Rowe and Kuroda (1965).

released at temperatures as low as 800 °C (Michel and Eugster, 1994) would have important implications for the origin of the achondrites. Such diverse achondrites as aubrites (Norton County), diogenites (Tatahouine), eucrites (Pasamonte), angrites (Angra dos Reis) and lodranites (Lodran) would carry a component that has not been observed in pure form in chondrites. However, most models that aim to explain the igneous formation of achondrites on their parent bodies start with chondritic material that is altered towards achondritic textures, chemical compositions and mineral assemblages. U-Xe must have survived severe conditions on the different parent bodies. These conditions include planetary processes such as (1) differentiation of the largely or completely molten initial Vesta at temperatures of ~1600 °C (howardite–eucrite–diogenite group meteorites (HED) parent body; see review by Drake, 2001); (2) partial or complete melting of enstatite chondrite material at ~1580 °C and possibly subsequent collisional disruption (aubrite parent body; Keil, 1989); (3) partial melting

of a chondritic precursor at temperatures of 950 to 1200 °C (Acapulcoite–Lodranite parent body; McCoy *et al.*, 1996, 1997a,b); (4) crystallization from basaltic magmas of partially melted carbonaceous chondrite-like material (Angrite parent body; Mittlefehldt *et al.*, 2002).

Regardless of the Xe isotopic composition, all these processes should lead to a significant loss of volatiles, as indicated, for example, in the generally small concentrations of trapped Xe in achondrites relative to chondrites, often overprinted by absorbed terrestrial Xe (see Table 6). The survival under such harsh conditions of significant amounts of U-Xe in certain samples is implausible, while Q gases, that are released between 1000 and 1600 °C (Huss *et al.*, 1996), are apparently absent in these samples but present in other achondrites of the same classes (Table 6).

It appears surprising that those achondrites, formed by crystallization of magma, still contain remnant primordial noble gases at all. Primitive achondrites, residues from partial melting processes, should more likely contain trapped gases. In fact, this is the case for the lodranites, acapulcoites and winonaites (Table 6). McCoy *et al.* (1996) suggested that the abundant noble gases in acapulcoites reflect the efficiency of retrapping of noble gases released during metamorphism. We infer from GRA 95209 and Lodran that this process might be effective as well for the lodranites. Possibly, Lodran experienced especially suitable conditions with temperatures high enough to form metal- and troilite-rich aggregates and low enough not to completely lose the trapped Xe.

A plausible mechanism to explain U-Xe in achondrites would be the formation of those achondrite classes mentioned above directly from the cooling nebula, a controversial model that has been suggested by Kurat (1988, 1990). However, this model can not easily explain the well-established genetic link of more primitive E chondritic precursor material and the differentiated aubrites (Keil, 1989). Additionally, the lack of other primitive constituents of the solar nebula such as presolar grains, chondrules, calcium-aluminum-rich inclusions (CAIs) and volatile-rich matrix or at least their isotopic signatures in achondrites does not support formation of these achondrite classes directly from the nebula.

IS XENON-Q A MIXTURE OF XENON-H AND U-XENON?

Although U-Xe may not be found in pure form in meteorites, its possible presence in the Earth could imply that the established meteoritic Xe components contain U-Xe. Based on stepwise heating measurements and the comparison with data from acid-resistant residues, Pepin and Phinney (1978) concluded that the trapped Xe components in bulk carbonaceous chondrites, which they identified as "Xe-H", "Xe-L" and U-Xe, already represent mixtures of precursor components. The authors suggested that these latter, more basic, components are inseparable by thermal analysis but visible in the residues. Xe-H and Xe-L are enriched in the heavy and light Xe isotopes, respectively, relative to the shielded isotope ^{130}Xe. It turned out later that the carrier phase of Xe-H (and Xe-L) is presolar diamonds (Lewis *et al.*, 1987). The second major carrier of trapped Xe in acid-resistant residues from carbonaceous chondrites is phase Q (Lewis *et al.*, 1975), a poorly defined enigmatic carrier (see also Busemann *et al.*, 2000; Huss *et al.*, 1996, and references therein).

We argue that Xe-HL from presolar diamonds and Xe-Q are sufficient to explain the data observed in bulk samples and residues from carbonaceous chondrites. The especially uniform occurrence of Xe-Q in different meteorite classes (Busemann *et al.*, 2000; Huss *et al.*, 1996) and the simultaneous release with He-Kr-Q suggests that Xe has not been mixed with significant amounts of Xe-H or any other Xe component. In a few cases, a redistribution of the HL component into the Q carrier during metamorphism has been observed (Huss *et al.*, 1996). This should result in the mixing of all noble gas elements of the Q and HL component. The process is discernible, for example, in the ^{20}Ne/^{22}Ne ratios intermediate between those of Q and HL. However, on line experiments have proven the uniform composition of Xe-Q and the general lack of Xe-HL in these samples, suggesting that Xe-Q and Xe-HL in meteorites are physically separable components with distinct compositions and origins. There is no need for U-Xe as a precursor component for meteoritic Xe. This does not exclude, however, that Xe-Q is a mixture of Xe-H and fractionated U-Xe that has been homogeneously mixed *prior* to the trapping into phase Q (Pepin and Phinney, 1978). In an almost identical approach, Lavielle and Marti (1992) suggested that Xe-Q in ordinary chondrites, which they call OC-Xe, might be a mixture of slightly fractionated solar wind and Xe-HL. However, both models need the separability of Xe-H and Xe-L, which has not been unambiguously achieved so far.

THE KRYPTON AND ARGON ISOTOPIC COMPOSITION

The Kr isotopic composition of Q and air is fractionated by only about 0.1–0.9%/amu relative to solar wind Kr favoring the heavier isotopes. All three components are possible constituents of the Kr in achondrites. However, the trapped Kr concentration in achondrites is in general small (Table 5) which leads to large statistic uncertainties while Kr_{cosm} significantly contributes to the total Kr. The exact determination of the trapped Kr component in achondrites is thus impossible in most cases.

The data points for the Lodran and GRA 95209 separates, Tatahouine, Shallowater and Mount Egerton scatter around the expected trapped compositions, whereas the data for the other aubrites, the angrites and Pasamonte lie on a trapped-cosmogenic-Kr mixing line (Fig. 9). Cumberland Falls and Mayo Belwa show large excesses of neutron-produced ^{80}Kr and ^{82}Kr. The spallation corrected data points for Shallowater indicate Q composition, whereas Norton County after correction

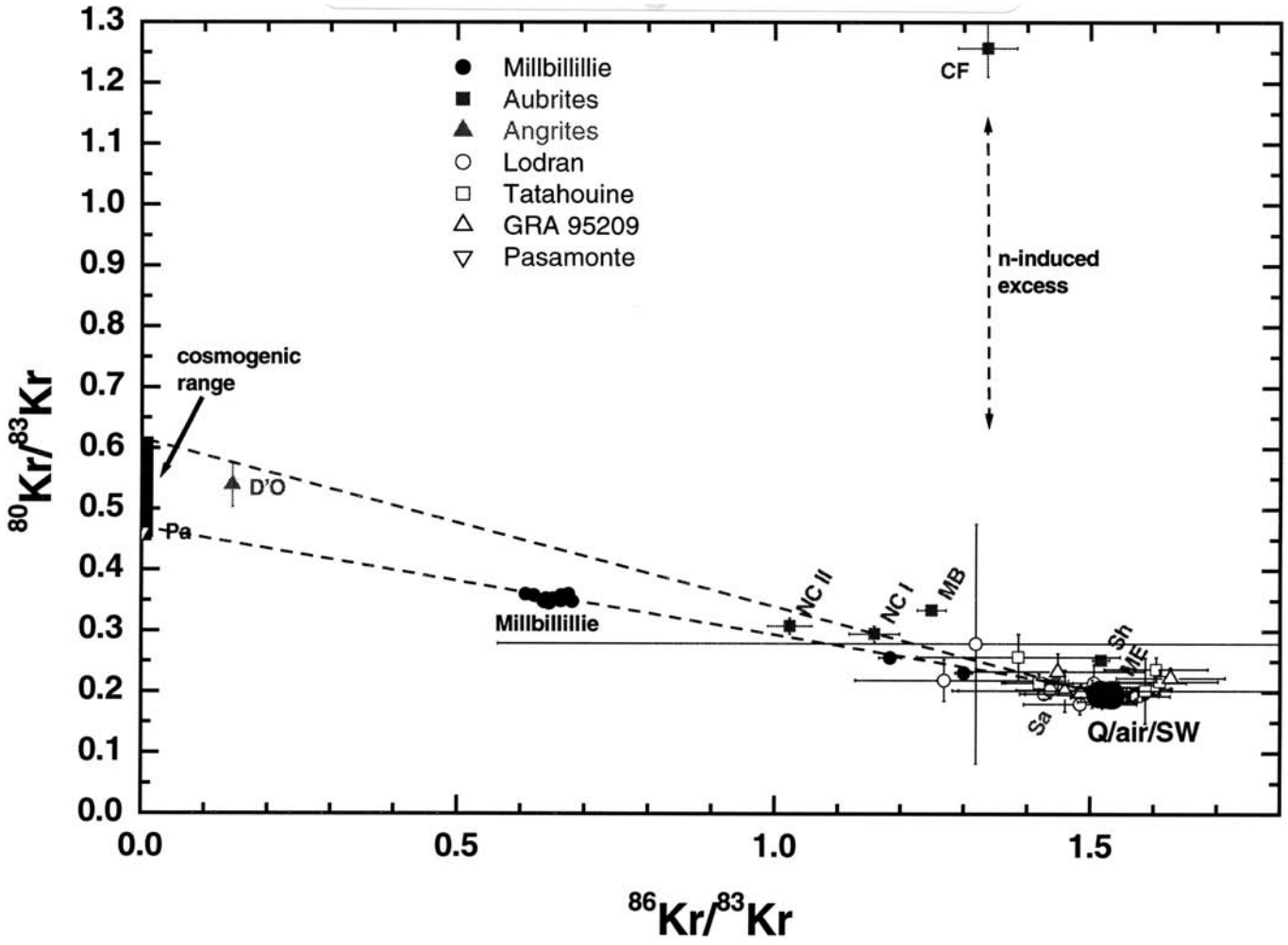

FIG. 9. The Kr isotopic composition in all samples is consistent with a mixture of cosmogenic Kr, n-produced ^{80,82}Kr (in some of the aubrites; see Lorenzetti *et al.*, 2002), fission Kr (D'Orbigny) and trapped Kr. The trapped Kr composition in all cases is close to Kr-Q or air.

plots close to air. All other aubrites contain mixtures of Kr-Q and air. Cosmogenic Kr and the n-induced production of ^{80}Kr and ^{82}Kr in the aubrites and angrites are discussed elsewhere (Eugster *et al.*, 2002; Lorenzetti *et al.*, 2002). All samples except for Pasamonte contain measurable amounts of $^{84}Kr_{tr}$. Especially large concentrations up to 3200×10^{-12} cm^3/g are found in the Lodran mineral separates. The concentrations exceed those for $^{132}Xe_{tr}$ and suggest that Xe has been trapped together with Kr. This implies that the arguable U-Xe in Lodran would be accompanied by "U-Kr".

The Ar isotopic composition in most of our measurements is dominated by cosmogenic ^{36}Ar and ^{38}Ar ($^{36}Ar/^{38}Ar < 2$; Tables 4 and A1) and radiogenic ^{40}Ar. $^{36}Ar/^{38}Ar$ ratios larger than ~2 indicate some trapped Ar. This is the case for the 800 °C steps of Tatahouine and Cumberland Falls, Shallowater and all Lodran separate measurements. Argon in the 800 °C steps of Tatahouine is air, as implied by the $^{40}Ar/^{36}Ar$ ratios and the low ^{36}Ar concentrations $<1 \times 10^{-8}$ cm^3/g in these steps. This is in agreement with the Xe isotope observations. The aubrites and Lodran separates contain significant $^{36}Ar_{tr}$ concentrations of $(1–80) \times 10^{-8}$ cm^3/g. The abundant trapped Kr and Xe concentrations in the Lodran metal-rich separates are accompanied by abundant trapped ^{36}Ar.

Surprisingly, the GRA 95209 Fe/Ni-rich sample contains radiogenic ^{40}Ar leading to $^{40}Ar/^{36}Ar$ ratios up to 5100 after correction for spallogenic Ar. Most of the ^{40}Ar is released at 1000 °C slightly earlier than the radiogenic ^{129}Xe at 1200 °C. The ^{40}Ar concentration in the Fe/Ni-rich separate is only 3–5× lower than that in the silicate-rich samples measured by Terribilini *et al.* (2000). This is too much $^{40}Ar_{rad}$ to be explainable with silicate inclusions within in the magnetic separate. We therefore infer that both radiogenic isotopes ^{40}Ar and ^{129}Xe are enriched in a mineral—or distinct minerals—associated with the metal. The earlier release of $^{40}Ar_{rad}$ relative to ^{129}Xe might be the result of the larger retentivity of Xe within a common carrier or it may indicate different carriers.

THE ELEMENTAL COMPOSITION

Finally, we discuss the elemental abundances of Ar and Kr relative to Xe. The discoverers of U-Xe did not discuss lighter noble gases that possibly accompany U-Xe. Nevertheless, a comparison of the trapped Ar/Xe and Kr/Xe ratios in the analysed achondrites with observations for chondrites (see, for example, Busemann *et al.*, 2000; Patzer and Schultz, 2002) might show hints at an additional (U-) Xe component (Fig. 10).

As already mentioned, the correction for $^{36}Ar_{cosm}$ often results in uncertainties of almost 100% for $^{36}Ar_{tr}$. For reasons of clarity, we thus do not show error bars in Fig. 10 and excluded data with uncertainties exceeding 100%. Nevertheless, Fig. 10 shows interesting trends. Most of those samples that contain large trapped gas concentrations (Lodran gas-rich samples) or only little terrestrial contamination (Cumberland Falls, Shallowater) plot close to a mixing line between the typical Q range (Busemann *et al.*, 2000) and the so-called subsolar composition. Subsolar gases (Crabb and Anders, 1981) have elemental and isotopic compositions intermediate between solar wind and Q gases. Q gases are strongly depleted in the lighter element or isotope relative to a heavier one when normalised to solar composition (Busemann *et al.*, 2002; Crabb and Anders, 1981). The subsolar gas composition of Ar-Xe is best represented in the E-chondrite South Oman (Crabb and Anders, 1981). The presence of subsolar gases in aubrites is easy to understand, because both aubrites and E chondrites accreted from similar E-chondritic precursor material (Keil, 1989). Therefore, we possibly measured some of the subsolar gas that remained after metamorphism. The Xe isotopic composition of our samples is close to Xe-Q, whereas the subsolar Xe isotopic composition might be, within large uncertainties, close to solar (Ott, 2002).

The samples of which the Xe isotopic composition already indicated terrestrial contamination such as Norton County, Tatahouine, GRA 95209 and the less gas-rich samples of Lodran almost exclusively plot, within the large uncertainties of their Ar/Xe ratios, close to or below the Q–air mixing line. Data

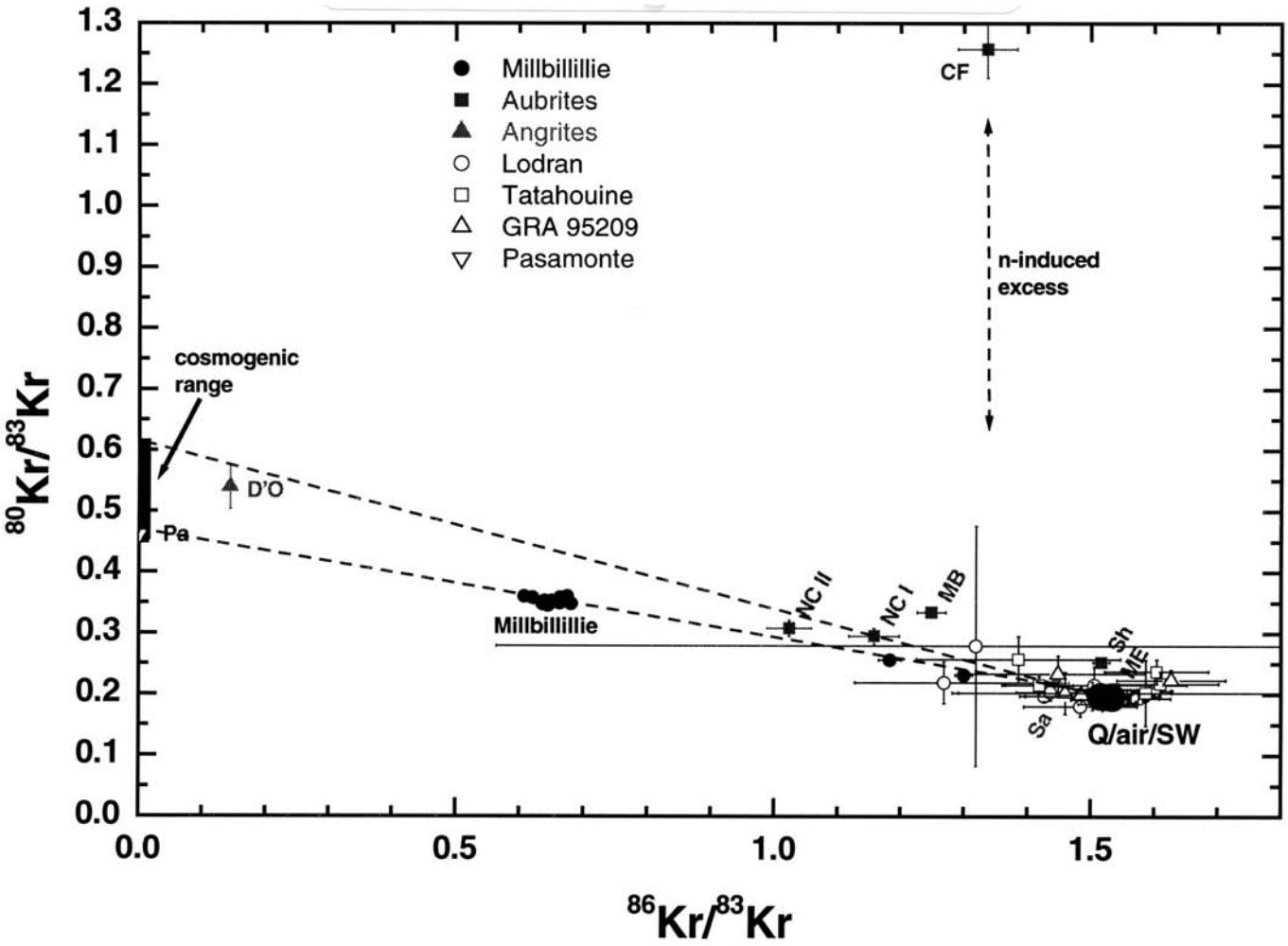

FIG. 10. The elemental composition of all samples after subtraction of the cosmogenic noble gases suggests that Lodran (gas-rich measurements) and the aubrites—in agreement with their close relation to the E chondrites—contain subsolar noble gases. The Millbillillie eucrite probably carries a trapped component more fractionated relative to Xe-Q or solar, while the gas-poor samples clearly trapped absorbed fractionated air.

points below this mixing line indicate the preferential absorption of terrestrial Kr and especially Xe. This effect has already been observed, for example, for weathered E and C chondrites (Crabb and Anders, 1981; Scherer and Schultz, 2000). The gas-rich Millbillillie samples also plot in the region below the Q–air mixing line. Samples #9 and #13 contain significant amounts of terrestrial contamination (Table A3 and Fig. 10), Xe in samples #2 and #4, however, do not indicate terrestrial contamination (Table A3). Their low Ar/Xe ratios could therefore hint at a different element composition of the originally trapped noble gases. The diogenite Tatahouine and the angrites are also "depleted" in Ar relative to Xe in Lodran or the aubrites, which thus could be a common property of the HED and angrite parent bodies. No data point plots to the lower left of the typical Q range, which suggests that there is no additional Xe component such as U-Xe.

CONCLUSION

Notwithstanding the "terrestrial Xe problem", which allows—or requires—the primitive U-Xe once incorporated into the accreting Earth (Pepin, 2000; see also Igarashi, 1995 for contrasting opinion), we conclude that achondritic meteorites do not indicate the presence of this Xe component. All data measured in this work and the measurements used to support the presence of a primitive Xe component other than Xe-Q in achondrites can straightforwardly be explained by mixtures of residual or retrapped Xe-Q, terrestrial Xe, and contributions of cosmogenic and fissiogenic Xe. The discrepancies observed cannot simply be the result of the use of a distinct set of cosmogenic Xe spectra. The striking gap between all data scattering around Xe-Q (or air) composition and U-Xe indicates that the compositions are not the result of mixtures of presolar Xe-H and U-Xe. The uniform occurrence of Xe-Q in different chondritic and achondritic meteorite classes and the homogeneous mixture with the other lighter noble gases suggests that Xe has not been mixed, independently from the other gases, with significant amounts of presolar Xe-H. Noble gases of Q composition must have been available during the accretion of the chondritic and achondritic parent bodies in similar composition. The Q composition is thus not the result of fractionation during metamorphism or loss of the early atmospheres on different bodies located throughout the asteroid-forming region of the solar system. However, this does not exclude the possibility that the Xe-Q composition might have established prior to the trapping in phase Q (*e.g.*, in the molecular cloud) by mixing of fractionated solar Xe and Xe-HL. The conclusion that achondrites contain trapped Xe of Q composition but no U-Xe sets constraints on the precursor material of the Earth. The primordial noble gases in the Earth resemble solar composition (or, in the case of the Xe isotopes, the closely related U-Xe). Consequently, the precursor material of the Earth was not mainly achondritic.

Acknowledgments–This work was supported by the Swiss National Science Foundation SNF. We gratefully acknowledge the technical support by A. Schaller and valuable discussions with M. Schönbächler, I. Tolstikhin, N. Vogel, and R. Wieler. Helpful reviews by J. Gilmour, K. Marti, and U. Ott are greatly appreciated. We thank T. Mikouchi (University of Tokyo) and the NASA meteorite working group for providing the Sahara 99555 sample, G. Kurat (Naturhistorisches Museum, Vienna) and M. E. Varela (Universidad Nacional de Sur, Bahia Blanca) for D'Orbigny, R. Hutchison (Natural History Museum, London) and G. Kurat for the Lodran samples and the NASA meteorite working group for GRA 95209.

Editorial handling: R. Wieler

REFERENCES

ALEXANDER E. C., JR., LEWIS R. S., REYNOLDS J. H. AND MICHEL M. C. (1971) Plutonium-244: Confirmation as an extinct radioactivity. *Science* **172**, 837–840.

BARRAT J. A., GILLET PH., LÉCUYER C., SHEPPARD S. M. F. AND LESOURD M. (1998) Formation of carbonates in the Tatahouine meteorite. *Science* **280**, 412–414.

BARRAT J. A., GILLET PH., LESOURD M., BLICHERT-TOFT J. AND POUPEAU G. R. (1999) The Tatahouine diogenite: Mineralogical and chemical effects of sixty-three years of terrestrial residence. *Meteorit. Planet. Sci.* **34**, 91–97.

BASFORD J. R., DRAGON J. C., PEPIN R. O., COSCIO M. R., JR. AND MURTHY V. R. (1973) Krypton and xenon in lunar fines. *Proc. Lunar Sci. Conf.* **4th**, 1915–1955.

BECKER R. H., SCHLUTTER D. J., RIDER P. E. AND PEPIN R. O. (1998) An acid-etch study of the Kapoeta achondrite: Implications for the argon-36/argon-38 ratio in the solar wind. *Meteorit. Planet. Sci.* **33**, 109–113.

BURGER M., EUGSTER O. AND KRÄHENBÜHL U. (1989) Refractory trace elements in different classes of achondrites by RNAA and INAA and some noble gas data (abstract). *Meteoritics* **24**, 256–257.

BUSEMANN H. AND EUGSTER O. (2000a) Primordial noble gases in Lodran metal separates and the Tatahouine diogenite (abstract). *Lunar Planet. Sci.* **31**, #1642, Lunar and Planetary Institute, Houston, Texas, USA (CD-ROM).

BUSEMANN H. AND EUGSTER O. (2000b) The search for U-Xe in achondrites: New data for xenon-rich Lodran metal and three aubrites (abstract). *Meteorit. Planet. Sci.* **35 (Suppl.)**, A37.

BUSEMANN H., BAUR H. AND WIELER R. (2000) Primordial noble gases in "Phase Q" in carbonaceous and ordinary chondrites studied by closed system stepped etching. *Meteorit. Planet. Sci.* **35**, 949–973.

BUSEMANN H., BAUR H. AND WIELER R. (2002) Phase Q—A carrier for subsolar noble gases (abstract). *Lunar Planet. Sci.* **33**, #1462, Lunar and Planetary Institute, Houston, Texas, USA (CD-ROM).

CRABB J. AND ANDERS E. (1981) Noble gases in E-chondrites. *Geochim. Cosmochim. Acta* **45**, 2443–2464.

DE LAETER J. R. AND HOSIE D. J. (1978) The abundance of barium in stony meteorites. *Earth Planet. Sci. Lett.* **38**, 416–420.

DRAKE M. J. (2001) The eucrite/Vesta story. *Meteorit. Planet. Sci.* **36**, 501–513.

EIKENBERG J., SIGNER P. AND WIELER R. (1993) U-Xe, U-Kr and U-Pb systematics for dating uranium minerals and investigations of the production of nucleogenic neon and argon. *Geochim. Cosmochim. Acta* **57**, 1053–1069.

EUGSTER O. AND MICHEL TH. (1995) Common asteroid break-up events of eucrites, diogenites, and howardites and cosmic-ray production rates for noble gases in achondrites. *Geochim. Cosmochim. Acta* **59**, 177–199.

EUGSTER O., EBERHARDT P. AND GEISS J. (1969) Isotopic analyses of krypton and xenon in fourteen stone meteorites. *J. Geophys. Res.* **74**, 3874–3896.

EUGSTER O., MICHEL TH. AND NIEDERMANN S. (1991) ^{244}Pu-Xe formation and gas retention age, exposure history, and terrestrial age of angrites LEW 86010 and LEW 87051: Comparison with Angra dos Reis. *Geochim. Cosmochim. Acta* **55**, 2957–2964.

EUGSTER O., BUSEMANN H., KURAT G., LORENZETTI S. AND VARELA M. E. (2002) Characterization of the noble gases and CRE age of the D'Orbigny angrite (abstract). *Meteorit. Planet. Sci.* **37 (Suppl.)**, A44.

FUKUOKA T. AND KIMURA M. (1990) Chemistry of Y-74063, -74357 and ALH-78230 unique meteorites. *Proc. NIPR Symp. Antarct. Meteorites* **15th**, 99–100.

GARRISON D. H. AND BOGARD D. D. (1997) ^{39}Ar-^{40}Ar ages and trapped and cosmogenic noble gases in Winonaite meteorites (abstract). *Lunar Planet. Sci.* **28**, 395–396.

GAST P. W., HUBBARD N. J. AND WIESMANN H. (1970) Chemical composition and petrogenesis of basalts from Tranquillity Base. *Proc. Apollo 11 Lunar Sci. Conf.* 1143–1163.

GILMOUR J. D., WHITBY J. A. AND TURNER G. (2001) Disentangling xenon components in Nakhla: Martian atmosphere, spallation and martian interior. *Geochim. Cosmochim. Acta* **65**, 343–354.

GRAHAM A. L. AND HENDERSON P. (1985) Rare earth element abundances in separated phases of Mayo Belwa, an enstatite achondrite. *Meteoritics* **20**, 141–149.

HOHENBERG C. M. (1970) Xenon from the Angra dos Reis meteorite. *Geochim. Cosmochim. Acta* **34**, 185–191.

HOHENBERG C. M., MUNK M. N. AND REYNOLDS J. H. (1967) Spallation and fissiogenic xenon and krypton from stepwise heating of the Pasamonte achondrite; The case for extinct plutonium 244 in meteorites; Relative ages of chondrites and achondrites. *J. Geophys. Res.* **72**, 3139–3177.

HOHENBERG C. M., HUDSON B., KENNEDY B. M. AND PODOSEK F. A. (1981) Xenon spallation systematics in Angra dos Reis. *Geochim. Cosmochim. Acta* **45**, 1909–1915.

HOHENBERG C. M., BERNATOWICZ T. J. AND PODOSEK F. A. (1991) Comparative xenonology of two angrites. *Earth Planet. Sci. Lett.* **102**, 167–177.

HUSS G. R. AND LEWIS R. S. (1994) Noble gases in presolar diamonds I: Three distinct components and their implications for diamond origins. *Meteoritics* **29**, 791–810.

HUSS G. R., LEWIS R. S. AND HEMKIN S. (1996) The "normal planetary" noble gas component in primitive chondrites: Compositions, carrier, and metamorphic history. *Geochim. Cosmochim. Acta* **60**, 3311–3340.

IGARASHI G. (1995) Primitive xenon in the earth. *AIP Conf. Proc.* **341**, 70–80.

JONES C. M., LUMPKIN G. R. AND REYNOLDS J. H. (1985) Trapped Xe components in etched samples of the Murray (C2) and Murchison (C2) carbonaceous chondrite. *Proc. Lunar Planet. Sci. Conf.* **15th**, *J. Geophys. Res.* **90 (Suppl.)**, C715–C721.

KEIL K. (1989) Enstatite meteorites and their parent bodies. *Meteoritics* **24**, 195–208.

KEIL K., NTAFLOS TH., TAYLOR G. J., BREARLEY A. J., NEWSOM H. E. AND ROMIG A. D., JR. (1989) The Shallowater aubrite: Evidence for origin by planetesimal impacts. *Geochim. Cosmochim. Acta* **53**, 3291–3307.

KIM Y., ZIPFEL J. AND MARTI K. (1995) Evolutionary trends in acapulcoites and lodranites: Evidence from N and Xe signatures (abstract). *Lunar Planet. Sci.* **26**, 751–752.

KURAT G. (1988) Primitive meteorites: An attempt towards unification. *Phil. Trans. Royal Soc. London A* **325**, 459–482.

KURAT G. (1990) Are igneous processes the only way to make differentiated meteorites (abstract). *Meteoritics* **25**, 377–378.

KURAT G., BRANDSTÄTTER F., CLAYTON R., NAZAROV M. A., PALME H., SCHULTZ L., VARELA M. E., WÄSCH E., WEBER H. W. AND WECKWERTH G. (2001) D'Orbigny: A new and unusual angrite (abstract). *Lunar Planet. Sci.* **32**, #1753, Lunar and Planetary Institute, Houston, Texas, USA (CD-ROM).

LAVIELLE B. AND MARTI K. (1992) Trapped xenon in ordinary chondrites. *J. Geophys. Res.* **97**, 20 875–20 881.

LEWIS R. S. (1975) Rare gases in separated whitlockite from the St. Severin chondrite: Xenon and krypton from fission of extinct ^{244}Pu. *Geochim. Cosmochim. Acta* **39**, 417–432.

LEWIS R. S., SRINIVASAN B. AND ANDERS E. (1975) Host phase of a strange xenon component in Allende. *Science* **190**, 1251–1262.

LEWIS R. S., MING T., WACKER J. F., ANDERS E. AND STEEL E. (1987) Interstellar diamonds in meteorites. *Nature* **326**, 160–162.

LEYA I., LANGE H-J., NEUMANN S., WIELER R. AND MICHEL R. (2000) The production of cosmogenic nuclides in stony meteoroids by galactic cosmic-ray particles. *Meteorit. Planet. Sci.* **35**, 259–286.

LODDERS K., PALME H. AND WLOTZKA F. (1993) Trace elements in mineral separates of the Peña Blanca Spring aubrite: Implications for the evolution of the aubrite parent body. *Meteoritics* **28**, 538–551.

LORENZETTI S., EUGSTER O., BUSEMANN H., MARTI K., BURBINE T. H. AND MCCOY T. (2002) History and origin of aubrites. *Geochim. Cosmochim. Acta* **37** (in press).

MAHAFFY P. R., NIEMANN H. B., ALPERT A., ATREYA S. K., DEMICK J., DONAHUE T. M., HARPOLD D. N. AND OWEN T. C. (2000) Noble gas abundance and isotope ratios in the atmosphere of Jupiter from the Galileo Probe Mass Spectrometer. *J. Geophys. Res.* **105**, 15 061–15 071.

MAKISHIMA A. AND MASUDA A. (1993) Primordial Ce isotopic composition of the solar system. *Chem. Geol.* **106**, 197–205.

MARTI K. AND LUGMAIR G. W. (1971) Kr^{81}-Kr and K-Ar^{40} ages, cosmic-ray spallation products, and neutron effects in lunar samples from Oceanus Procellarum. *Proc. Lunar Planet. Sci. Conf.* **2nd**, 1591–1605.

MARTI K., EBERHARDT P. AND GEISS J. (1966) Spallation, fission, and neutron capture anomalies in meteoritic krypton and xenon. *Z. Naturforschung* **21a**, 398–413.

MASON B. AND JAROSEWICH E. (1971) The composition of the Johnstown meteorite. *Meteoritics* **6**, 241–245.

MASUDA A. AND TANAKA T. (1978) REE, Ba, Sr and Rb in the Yamato meteorites, with special reference to Yamato-691(a), -692(b) and -693(c). *Proc. Symp. Yamato Meteorites* **2nd**, 229–232.

MATHEW K. J. AND BEGEMANN F. (1995) Isotopic composition of xenon and krypton in silicate-graphite inclusions of the El Taco, Campo del Cielo, IAB iron meteorite. *Geochim. Cosmochim. Acta* **59**, 4729–4746.

MATHEW K. J., RAO M. N., WEBER H. W., HERPERS U. AND MICHEL R. (1994) Xenon production cross sections at intermediate energies and production rates in small meteoroids based on simulation experiments. *Nucl. Instrum. Methods Phys. Res. B* **94**, 449–474.

MCCARTHY T. S., ERLANK A. J. AND WILLIS J. P. (1973) On the origin of eucrites and diogenites. *Earth Planet. Sci. Lett.* **18**, 433–442.

MCCOY T. J., KEIL K., CLAYTON R. N., MAYEDA T. K., BOGARD D. D., GARRISON D. H., HUSS G. R., HUTCHEON I. D. AND WIELER R. (1996) A petrologic, chemical, and isotopic study of Monument Draw and comparison with other acapulcoites: Evidence for formation by incipient partial melting. *Geochim. Cosmochim. Acta* **60**, 2681–2708.

MCCOY T. J., KEIL K., CLAYTON R. N., MAYEDA T. K., BOGARD D. D., GARRISON D. H. AND WIELER R. (1997a) A petrologic and isotopic study of lodranites: Evidence for early formation as partial melt residues from heterogeneous precursors. *Geochim. Cosmochim. Acta* **61**, 623–637.

McCoy T. J., Keil K., Muenow D. W. and Wilson L. (1997b) Partial melting and melt migration in the acapulcoite-lodranite parent body. *Geochim. Cosmochim. Acta* **61**, 639–650.

Michel Th. and Eugster O. (1994) Primitive xenon in diogenites and plutonium-244-fission xenon ages of a diogenite, a howardite, and eucrites. *Meteoritics* **29**, 593–606.

Mittlefehldt D. W. (1979) Petrographic and chemical characterization of igneous lithic clasts from mesosiderites and howardites and comparison with eucrites and diogenites. *Geochim. Cosmochim. Acta* **43**, 1917–1935.

Mittlefehldt D. W. and Lindstrom M. M. (1990) Geochemistry and genesis of the angrites. *Geochim. Cosmochim. Acta* **54**, 3209–3218.

Mittlefehldt D. W., Lindstrom M. M., Bogard D. D., Garrison D. H. and Field S. W. (1996) Acapulco- and Lodran-like achondrites: Petrology, geochemistry, chronology, and origin. *Geochim. Cosmochim. Acta* **60**, 867–882.

Mittlefehldt D. W., Killgore M. and Lee M. T. (2002) Petrology and geochemistry of D'Orbigny, geochemistry of Sahara 99555, and the origin of angrites. *Meteorit. Planet. Sci.* **37**, 345–369.

Miura Y., Nagao K. and Fujitani T. (1993) ^{81}Kr terrestrial ages and grouping of Yamato eucrites based on noble gas and chemical composition. *Geochim. Cosmochim. Acta* **57**, 1857–1866.

Miura Y. N., Nagao K. and Okazaki R. (1999) Noble gases in five aubrites, Cumberland Falls, Mayo Belwa, Mt. Egerton, Norton County and Peña Blanca Spring. *Antarct. Meteorites* **24**, 108–110.

Moore C. B. and Brown H. (1963) Barium in stony meteorites. *J. Geophys. Res.* **68**, 4293–4296.

Munk M. N. (1967) Argon, krypton, and xenon in Angra dos Reis, Nuevo Laredo, and Norton County achondrites: The case for two types of fission Xe in achondrites. *Earth Planet. Sci. Lett.* **3**, 457–465.

Nagao K. and Miura Y. N. (1994) Trapped Xe component in a silicate phase of the Brenham pallasite (abstract). *Meteoritics* **29**, 509.

Nagao K., Eugster O., Weigel A., Miura Y. N., Koeberl C. and Takaoka N. (1995) Noble gases, chemical composition, and cosmic-ray exposure age of the Yamato-74357 lodranite. *Proc. NIPR Symp. Antarct. Meteorites* **8**, 297–303.

Niedermann S. and Eugster O. (1992) Noble gases in lunar anorthositic rocks 60018 and 65315: Acquisition of terrestrial krypton and xenon indicating an irreversible adsorption process. *Geochim. Cosmochim. Acta* **56**, 493–509.

Niemeyer S. and Zaikowski A. (1980) I-Xe age and trapped Xe components of the Murray (C-2) chondrite. *Earth Planet. Sci. Lett.* **48**, 335–347.

Nyquist L. E., Bansal B., Wiesmann H. and Shih C-Y. (1994) Neodymium, strontium and chromium isotopic studies of the LEW 86010 and Angra dos Reis meteorites and the chronology of the angrite parent body. *Meteoritics* **29**, 872–885.

Ott U. (1988) Noble gases in SNC meteorites: Shergotty, Nakhla, Chassigny. *Geochim. Cosmochim. Acta* **52**, 1937–1948.

Ott U. (2002) Noble gases in meteorites—Trapped components. *Rev. Mineral. Geochem.* **47**, 71–100.

Ott U., Löhr H. P. and Begemann F. (1993) Noble gases in Yamato-75097 inclusion: Similarities to Brachinites (only?). *Proc. Symp. Antarct. Meteorites* **18th**, 236–239.

Owen T., Bar-Nun A. and Kleinfeld I. (1992) Possible cometary origin of heavy noble gases in the atmospheres of Venus, Earth and Mars. *Nature* **358**, 43–46.

Owen T., Mahaffy P., Niemann H. B., Atreya S., Donahue T., Bar-Nun A. and de Pater I. (1999) A low-temperature origin for the planetesimals that formed Jupiter. *Nature* **402**, 269–270.

Ozima M. and Podosek F. A. (2002) *Noble Gas Geochemistry*. Cambridge Univ. Press, Cambridge, U.K. 286 pp.

Palme H. and Beer H. (1993) Abundances of the elements in the solar system. In *Astronomy and Astrophysics* (ed. H. H. Voigt), pp. 196–221. Springer, Berlin, Germany.

Palme H., Schultz L., Spettel B., Weber H. W., Wänke H., Christophe Michel-Levy M. and Lorin J. C. (1981) The Acapulco meteorite: Chemistry, mineralogy and irradiation effects. *Geochim. Cosmochim. Acta* **45**, 727–752.

Patzer A. and Schultz L. (2002) Noble gases in enstatite chondrites II: The trapped component. *Meteorit. Planet. Sci.* **37**, 601–612.

Pepin R. O. (1992) Origin of noble gases in the terrestrial planets. *Ann. Rev. Earth Planet. Sci.* **20**, 389–430.

Pepin R. O. (2000) On the isotopic composition of primordial xenon in terrestrial planet atmospheres. *Space Sci. Rev.* **92**, 371–395.

Pepin R. O. and Phinney D. (1978) Components of xenon in the solar system. *unpublished preprint,* University of Minnesota, Minneapolis, USA.

Pepin R. O., Becker R. H. and Rider P. E. (1995) Xenon and krypton isotopes in extraterrestrial regolith soils and in the solar wind. *Geochim. Cosmochim. Acta* **59**, 4997–5022.

Porcelli D. and Pepin R. O. (2000) Rare gas constraints on early earth history. In *Origin of the Earth and Moon* (eds. R. M. Canup and K. Righter), pp. 435–458. Univ. Arizona Press, Tucson, Arizona, USA.

Rowe M. W. and Bogard D. D. (1966) Isotopic composition of xenon from Ca-poor achondrites. *J. Geophys. Res.* **71**, 4183–4188.

Rowe M. W. and Kuroda P. K. (1965) Fissiogenic xenon from the Pasamonte meteorite. *J. Geophys. Res.* **70**, 709–714.

Rowe M. W., Bogard D. D. and Manuel O. K. (1965) Noble gases from the Peace River, LaLande and Achilles meteorites. *Geochim. Cosmochim. Acta* **29**, 1199–1202.

Scherer P. and Schultz L. (2000) Noble gas record, collisional history, and pairing of CV, CO, CK and other carbonaceous chondrites. *Meteorit. Planet. Sci.* **35**, 145–153.

Schultz L. and Kruse H. (2000) He, Ne and Ar in meteorites—A data collection. MPI für Chemie, Mainz, Germany (CD-ROM).

Shimizu H. and Masuda A. (1981) REE, Ba, Sr and Rb abundances in some unique antarctic achondrites. *Proc. NIPR Symp. Antarct. Meteorites* **6th**, 211–220.

Shimizu H. and Masuda A. (1982) REE characteristics of Antarctic eucrites. *Proc. NIPR Symp. Antarct. Meteorites* **7th**, 145–152.

Shimizu H. and Masuda A. (1986) REE patterns of eucrites and their genetic implications. *Geochim. Cosmochim. Acta* **50**, 2453–2460.

Shukolyukov A. and Begemann F. (1996a) Cosmogenic and fissiogenic noble gases and ^{81}Kr-Kr exposure age clusters of eucrites. *Meteorit. Planet. Sci.* **31**, 60–72.

Shukolyukov A. and Begemann F. (1996b) Pu-Xe dating of eucrites. *Geochim. Cosmochim. Acta* **60**, 2453–2471.

Shukolyukov Y. A., Assonov S. S., Smoliar M. I. and Kolesnikov E. M. (1995) Noble gases and strontium isotopes in the unique meteorite Divnoe. *Meteoritics* **30**, 654–660.

Swindle T. D., Kring D. A., Burkland M. K., Hill D. H. and Boynton W. V. (1998) Noble gases, bulk chemistry, and petrography of olivine-rich achondrites Eagles Nest and Lewis Cliff 88763: Comparison to brachinites. *Meteorit. Planet. Sci.* **33**, 31–48.

Takaoka N. (1972) An interpretation of general anomalies of xenon and the isotopic composition of primitive xenon. *Mass Spectr. (Shitsuryo Bunseki)* **20**, 287–302.

Takaoka N., Nagao K. and Miura Y. (1993) Noble gases in the unique meteorites Yamato-74063 and -74357. *Proc. NIPR Symp. Antarct. Meteorites* **6**, 120–134.

Tera F., Eugster O., Burmett D. S. and Wasserburg G. J. (1970) Comparative study of Li, Na, K, Rb, Cs, Ca, Sr and Ba abundances in achondrites and in Apollo 11 lunar samples. *Proc. Apollo 11 Lunar Sci. Conf.*, 1637–1657.

TERRIBILINI D. (2000) Edelgasisotopenanalysen und Bestrahlungsgeschichte von extraterrestrischen Gesteins- und Metallproben. Dissertation thesis. University of Bern, Bern, Switzerland. 205 pp.

TERRIBILINI D., EUGSTER O., HERZOG G. F. AND SCHNABEL C. (2000) Evidence for common breakup events of the acapulcoites-lodranites and chondrites. *Meteorit. Planet. Sci.* **35**, 1043–1050.

TORIGOYE N., YAMAMOTO K., MISAWA K. AND NAKAMURA N. (1993) Compositions of REE, K, Rb, Sr, Ba, Mg, Ca, Fe, and Sr isotopes in Antarctic "unique" meteorites. *Proc. NIPR Symp. Antarct. Meteorites* **6**, 100–119.

VOGEL N., BAUR H., BISCHOFF A. AND WIELER R. (2002) Noble gases in chondrules and metal-sulfide rims of primitive chondrites—Clues on chondrule formation (abstract). *Geochim. Cosmochim. Acta* **66**, A809.

WÄNKE H. *ET AL.* (1977) On the chemistry of lunar samples and achondrites. Primary matter in the lunar highlands: A re-evaluation. *Proc. Lunar Sci. Conf.* **8th**, 2191–2213.

WARREN P. H., KALLEMEYN G. W. AND MAYEDA T. (1995) Consortium investigation of the Asuka-881371 angrite: Bulk-rock geochemistry and oxygen isotopes. *Antarct. Meteorites* **20**, 261–264.

WEIGEL A. (1996) Untersuchung der Entstehungsgeschichte von Achondriten anhand von Edelgas-Isotopenanalysen sowie Entwicklung eines Extraktions-, Reinigungs- und Analysesystems für Stickstoff. Dissertation thesis. University of Bern, Bern, Switzerland. 91 pp.

WEIGEL A. AND EUGSTER O. (1994) Primitive trapped Xe in Lodran minerals and further evidence from EET 84302 and Gibson for break-up of the lodranite parent asteroid 4 Ma ago (abstract). *Lunar Planet. Sci. Conf.* **25**, 1479–1480.

WEIGEL A., EUGSTER O., KOEBERL C. AND KRÄHENBÜHL U. (1997) Differentiated achondrites Asuka 881371, an angrite, and Divnoe: Noble gases, ages, chemical composition, and relation to other meteorites. *Geochim. Cosmochim. Acta* **61**, 239–248.

WEIGEL A., EUGSTER O., KOEBERL C., MICHEL R., KRÄHENBÜHL U. AND NEUMANN S. (1999) Relationships among lodranites and acapulcoites: Noble gas isotopic abundances, chemical composition, cosmic-ray exposure ages, and solar cosmic ray effects. *Geochim. Cosmochim. Acta* **63**, 175–192.

WHITBY J. A., BUSEMANN H., EUGSTER O., HOLLAND G. AND GILMOUR J. D. (2002) I-Xe analysis of a magnetic separate from lodranite GRA 95209 (abstract). *Lunar Planet. Sci.* **33**, #1838, Lunar and Planetary Institute, Houston, Texas, USA (CD-ROM).

WIELER R. (2002) Noble gases in the solar system. *Rev. Mineral. Geochem.* **47**, 21–70.

WOLF R., EBIHARA M., RICHTER G. R. AND ANDERS E. (1983) Aubrites and diogenites: Trace element clues to their origin. *Geochim. Cosmochim. Acta* **47**, 2257–2270.

ZAHNLE K. (1993) Planetary noble gases. In *Protostars and Planets III* (eds. E. H. Levy and J. I. Lunine), pp. 1305–1338. Univ. Arizona Press, Tucson, Arizona, USA.

ZÄHRINGER J. (1968) Rare gases in stony meteorites. *Geochim. Cosmochim. Acta* **32**, 209–237.

APPENDIX

TABLE A1. Ar concentrations and isotopic composition in Millbillillie and two angrites.

		^{40}Ar (10^{-8} cm^3/g)	$^{36}Ar/^{38}Ar$	$^{40}Ar/^{36}Ar$	$^{36}Ar_{tr}$ (10^{-8} cm^3/g)	$^{38}Ar_{cosm}$ (10^{-8} cm^3/g)
Millbillillie	#1 (8/1999)	1345 ± 188	0.670 ± 0.012	542 ± 11	b.d.	3.684 ± 0.016
	#2 (8/1999)	1259 ± 134	0.725 ± 0.028	504 ± 20	0.29 ± 0.29	3.388 ± 0.015
	#3 (9/1999)	1282 ± 126	0.688 ± 0.013	520 ± 10	b.d.	3.548 ± 0.016
	#4 (4/2000)	1065 ± 103	0.727 ± 0.007	504 ± 7	0.25 ± 0.22	2.860 ± 0.013
	#5 (7/2000)	1274 ± 216	0.729 ± 0.012	502 ± 9	b.d.	3.417 ± 0.016
	#6 (7/2000)	1287 ± 227	0.714 ± 0.009	517 ± 8	b.d.	3.441 ± 0.016
	#7 (7/2000)	1260 ± 223	0.717 ± 0.011	508 ± 9	b.d.	3.412 ± 0.015
	#8 (2/2001)	1534 ± 1569	0.701 ± 0.012	543 ± 8	b.d.	3.983 ± 0.018
	#9 (7/2001)	1549 ± 213*	0.988 ± 0.038*	455 ± 11*	1.3 ± 0.5	3.192 ± 0.017
	#10 (7/2001)	1322 ± 181	0.698 ± 0.006	516 ± 6	b.d.	3.636 ± 0.016
	#11 (12/2001)	1170 ± 119	0.667 ± 0.013	554 ± 7	b.d.	3.154 ± 0.014
	#12 (1/2002)	1204 ± 124	0.672 ± 0.014	542 ± 7	b.d.	3.290 ± 0.014
	#13 (1/2002)†	1342 ± 141*	1.003 ± 0.030*	491 ± 4*	1.09 ± 0.29	2.519 ± 0.014
	Average	**1273 ± 35**	**0.701 ± 0.007**	**520 ± 6**	b.d.	**3.35 ± 0.10**
	Bern analog 1995‡	1383 ± 120	0.662 ± 0.010	557 ± 10	–	–
	Bern analog 1996–2000§	1309 ± 20	0.66 ± 0.04	556 ± 2	–	–
Sahara 99555		268 ± 90	0.984 ± 0.010	151.2 ± 2.0	b.d.	1.669 ± 0.009
D'Orbigny		57 ± 3	0.679 ± 0.005	33.5 ± 0.4	b.d.	2.486 ± 0.011

*Large atmospheric Ar contributions, excluded from average calculation.

†Fusion crust.

‡Average of four measurements (Eugster and Michel, 1995).

§Average of eight measurements with the MAP 215 mass spectrometer and analogue technique (Terribilini, 2000).

b.d. = below detection limit.

TABLE A2. Kr concentrations and isotopic composition in Millbillillie and two angrites.

	^{86}Kr (10^{-12} cm^3/g)	^{78}Kr/^{86}Kr	^{80}Kr/^{86}Kr	^{81}Kr/^{86}Kr	^{82}Kr/^{86}Kr	^{83}Kr/^{86}Kr	^{84}Kr/^{86}Kr	^{83}Kr$_{cosm}$ (10^{-12} cm^3/g)	^{84}Kr$_{tr}$ (10^{-12} cm^3/g)
Millbillillie									
#1 (8/1999)	17.7 ± 1.7	15.62 ± 0.17	53.8 ± 0.5	0.721 ± 0.016	129.8 ± 1.7	150.6 ± 1.6	369 ± 6	15.11 ± 0.14	55.9 ± 1.1
#2 (8/1999)	18.4 ± 1.7	15.6 ± 0.3	51.1 ± 0.6	0.71 ± 0.05	124.2 ± 1.6	147.0 ± 2.2	372 ± 5	15.03 ± 0.14	59.0 ± 0.9
#3 (9/1999)	16.2 ± 1.9	16.5 ± 0.4	57.6 ± 0.8	0.80 ± 0.05	135 ± 3	161 ± 3	368 ± 15	15.54 ± 0.14	49.8 ± 2.4
#4 (4/2000)	16.2 ± 1.5	15.55 ± 0.17	52.6 ± 0.5	0.660 ± 0.028	130.1 ± 1.3	150.9 ± 1.5	372 ± 5	13.86 ± 0.13	51.5 ± 0.8
#5 (7/2000)	15.6 ± 1.7	15.88 ± 0.28	54.6 ± 1.2	0.773 ± 0.019	136 ± 3	157 ± 3	366 ± 12	14.37 ± 0.13	48.1 ± 1.8
#6 (7/2000)	16.5 ± 1.7	15.58 ± 0.23	53.3 ± 0.6	0.796 ± 0.010	127.7 ± 2.0	148.2 ± 2.0	364 ± 9	13.72 ± 0.13	51.6 ± 1.5
#7 (7/2000)	15.9 ± 1.8	15.15 ± 0.27	52.9 ± 0.9	0.702 ± 0.012	128 ± 3	151 ± 3	363 ± 13	13.64 ± 0.13	49.1 ± 2.1
#8 (2/2001)	20.5 ± 1.4	16.0 ± 0.3	55.1 ± 1.0	0.80 ± 0.05	132.3 ± 1.9	156.4 ± 2.4	373 ± 7	18.67 ± 0.17	64.7 ± 1.3
#9 (7/2001)	116 ± 7*	4.80 ± 0.04*	21.62 ± 0.15*	0.160 ± 0.004*	80.6 ± 0.5*	84.6 ± 0.5*	339.5 ± 1.9*	22.0 ± 0.5	379 ± 7*
#10 (7/2001)	28.6 ± 1.8	14.78 ± 0.24	52.2 ± 0.9	0.732 ± 0.020	127.7 ± 2.0	148.1 ± 2.6	370 ± 7	23.72 ± 0.23	91.0 ± 2.0
#11 (12/2001)	19.1 ± 0.4	15.86 ± 0.28	53.4 ± 0.8	0.701 ± 0.021	132.3 ± 1.4	155.0 ± 2.1	370 ± 4	17.18 ± 0.16	59.8 ± 0.8
#12 (1/2002)	16.1 ± 0.4	17.43 ± 0.23	59.1 ± 0.7	0.905 ± 0.018	138.4 ± 1.5	164.3 ± 1.7	377 ± 4	16.5 ± 0.5	50.3 ± 0.7
#13 (1/2002)†	143 ± 4*	3.82 ± 0.05*	17.77 ± 0.18*	0.0881 ± 0.0021*	74.8 ± 0.8*	76.9 ± 0.8*	333.6 ± 2.6*	16.3 ± 0.6	467 ± 4*
Average	**18.3 ± 1.1**	**15.82 ± 0.21**	**54.2 ± 0.7**	**0.756 ± 0.021**	**131.0 ± 1.3**	**153.6 ± 1.7**	**369.3 ± 1.3**	**16.6 ± 0.9**	**57 ± 4**
Bern analog 1995‡	21 ± 4	13.9 ± 0.4	50.2 ± 2.0	0.64 ± 0.05	124 ± 4	143 ± 3	369 ± 2	–	–
Mainz 1996§	17.8 ± 1.8	14.64 ± 0.09	51.4 ± 0.4	0.57 ± 0.04	123.9 ± 0.6	142.4 ± 0.6	362.3 ± 1.3	–	–
Bern analog 1996–2000#	23.5 ± 1.3	13.7 ± 1.3	49 ± 4	0.64 ± 0.07	122 ± 6	142 ± 8	365 ± 5	–	–
Sahara 99555	146 ± 10	2.84 ± 0.05	15.11 ± 0.22	0.0781 ± 0.0026	68.4 ± 0.9	69.2 ± 1.0	327 ± 5	5.2 ± 0.6	476 ± 7
D'Orbigny$	2.0 ± 0.4	143 ± 6	374 ± 17	9.0 ± 0.5	573 ± 9	695 ± 34	574 ± 72	12.96 ± 0.07	5.8 ± 1.8

Isotopic ratios normalised to ^{86}Kr = 100.

*Large atmospheric Kr contributions, excluded from average calculation.

†Fusion crust.

‡Average of two measurements (Eugster and Michel, 1995).

§Shukolyukov and Begemann (1996a).

#Average of eight measurements with the MAP 215 mass spectrometer and analogue technique (Terribilini, 2000).

$Blank correction >20% of the measured ^{86}Kr.

TABLE A3. Xe concentrations and isotopic composition in Millbillillie and two angrites.

Sample	^{132}Xe (10^{-12} cm^3/g)	^{124}Xe/^{132}Xe	^{126}Xe/^{132}Xe	^{128}Xe/^{132}Xe	^{129}Xe/^{132}Xe	^{130}Xe/^{132}Xe	^{131}Xe/^{132}Xe	^{134}Xe/^{132}Xe	^{136}Xe/^{132}Xe	^{132}Xe$_{tr}$ (10^{-12} cm^3/g)	^{126}Xe$_{cosm}$ (10^{-12} cm^3/g)	^{136}Xe$_f$* (10^{-12} cm^3/g)
Millbillillie												
#1	44 ± 4	1.81 ± 0.07	2.96 ± 0.07	10.15 ± 0.11	93.1 ± 0.7	16.72 ± 0.17	89.7 ± 0.5	43.80 ± 0.24	39.2 ± 0.3	39 ± 9	1.166 ± 0.018	5 ± 5
#2	20.9 ± 1.1	2.24 ± 0.14	3.62 ± 0.15	11.6 ± 0.5	88.1 ± 2.5	16.3 ± 0.7	88.4 ± 2.2	43.8 ± 0.9	39.2 ± 0.8	17 ± 4	0.692 ± 0.007	3.0 ± 2.0
#3	26.1 ± 2.3	2.14 ± 0.03	3.77 ± 0.10	12.24 ± 0.24	90.7 ± 1.4	17.0 ± 0.4	92.7 ± 1.2	45.9 ± 0.6	42.6 ± 0.7	22 ± 6	0.896 ± 0.010	4.4 ± 2.6
#4	34.7 ± 1.8	2.17 ± 0.03	3.65 ± 0.05	11.39 ± 0.13	91.0 ± 0.7	15.74 ± 0.15	91.0 ± 0.5	45.39 ± 0.29	40.9 ± 0.4	27 ± 7	1.163 ± 0.011	6 ± 3
#5	30.7 ± 1.8	2.29 ± 0.04	3.86 ± 0.05	11.78 ± 0.12	91.9 ± 0.9	17.22 ± 0.17	93.5 ± 0.7	44.1 ± 0.4	41.0 ± 0.4	26 ± 7	1.088 ± 0.009	5 ± 3
#6	31.7 ± 1.5	2.21 ± 0.03	3.76 ± 0.04	11.27 ± 0.18	92.2 ± 0.9	17.31 ± 0.20	93.1 ± 0.7	45.0 ± 0.4	41.1 ± 0.4	28 ± 7	1.095 ± 0.013	5 ± 3
#7	32.2 ± 1.8	2.00 ± 0.03	3.42 ± 0.04	10.89 ± 0.15	92.1 ± 1.5	16.9 ± 0.3	90.5 ± 1.2	44.6 ± 0.7	39.9 ± 0.6	28 ± 7	1.001 ± 0.012	4 ± 3
#8	32.9 ± 1.2	1.97 ± 0.05	3.51 ± 0.08	11.87 ± 0.21	91.6 ± 1.7	17.1 ± 0.4	92.6 ± 1.8	46.1 ± 1.1	41.2 ± 0.9	29 ± 7	1.042 ± 0.011	5 ± 3
#9	49 ± 8†	1.77 ± 0.07†	3.02 ± 0.04†	10.25 ± 0.25†	96.3 ± 1.8†	16.7 ± 0.5†	89.5 ± 2.1†	42.4 ± 0.9†	37.9 ± 0.7†	43 ± 10†	1.336 ± 0.020	6 ± 5
#10	31 ± 5	1.97 ± 0.06	3.57 ± 0.10	11.2 ± 0.3	92.6 ± 2.4	17.2 ± 0.5	92.5 ± 2.3	43.8 ± 1.0	39.3 ± 0.9	27 ± 7	1.013 ± 0.011	4 ± 3
#11	36.5 ± 1.1	2.20 ± 0.03	3.67 ± 0.05	11.34 ± 0.16	90.1 ± 1.0	17.03 ± 0.17	92.1 ± 0.6	44.7 ± 0.4	40.3 ± 0.4	31 ± 8	1.228 ± 0.012	5 ± 4
#12	29.3 ± 0.5	2.37 ± 0.04	3.85 ± 0.05	11.68 ± 0.13	89.5 ± 1.0	17.27 ± 0.17	92.9 ± 0.6	46.0 ± 0.4	41.8 ± 0.4	25 ± 6	1.037 ± 0.009	5 ± 3
#13‡	90.7 ± 1.4†	1.096 ± 0.016†	1.641 ± 0.020†	8.75 ± 0.08†	96.3 ± 0.9†	16.03 ± 0.10†	82.4 ± 0.5†	41.4 ± 0.3†	36.6 ± 0.3†	84 ± 18†	1.18 ± 0.03	8 ± 9†
Average	**30.6 ± 1.4**	**2.16 ± 0.04**	**3.67 ± 0.05**	**11.53 ± 0.12**	**91.0 ± 0.4**	**16.88 ± 0.15**	**91.7 ± 0.5**	**44.81 ± 0.27**	**40.6 ± 0.3**	**27.3 ± 1.6**	**1.07 ± 0.04**	**4.73 ± 0.23**
Bern analog												
1995§	42 ± 6	1.63 ± 0.04	2.66 ± 0.07	10.3 ± 0.4	93.7 ± 1.0	16.4 ± 0.3	86.0 ± 1.7	42.6 ± 0.4	37.4 ± 0.4	–	–	2.83 ± 0.45
Mainz#	32.9	2.27 ± 0.03	3.77 ± 0.04	11.6 ± 0.1	91.1 ± 0.4	16.8 ± 0.1	86.4 ± 0.4	45.0 ± 0.2	41.3 ± 0.1	–	–	4.3 ± 0.5§
Bern analog												
1996–2000$	33.0 ± 2.2	1.93 ± 0.07	3.18 ± 0.09	10.98 ± 0.09	92.8 ± 2.6	16.87 ± 0.15	89.9 ± 0.9	44.7 ± 0.5	40.3 ± 0.5	–	–	–
Sahara 99555	79.1 ± 2.6	0.638 ± 0.018	0.695 ± 0.012	7.02 ± 0.12	90.8 ± 0.9	14.08 ± 0.19	75.0 ± 0.8	45.1 ± 0.5	40.1 ± 0.5	69 ± 15	0.295 ± 0.021	11 ± 8
D'Orbigny@	16.9 ± 2.2	3.20 ± 0.27	5.3 ± 0.5	10.0 ± 0.9	47 ± 5	9.9 ± 1.1	56 ± 6	79 ± 7	84 ± 7	5.4 ± 1.7	0.8816 ± 0.0028	12.4 ± 1.4

Isotopic ratios normalised to ^{132}Xe ≡ 100.

*Based on ^{130}Xe, large uncertainties because we used $(^{136}Xe/^{130}Xe)_{tr}$ with an uncertainty that covers U, air and Q composition.

†Large atmospheric Xe contributions, excluded from average calculation.

‡Fusion crust.

§Average of two measurements (Eugster and Michel, 1995).

#Shukolyukov and Begemann (1996b).

$Average of eight measurements with the MAP 215 mass spectrometer and analogue technique (Terribilini, 2000).

@Large uncertainties most likely due to sensitivity variations during the measurement caused by unsufficient removal of reactive gases.

TABLE A4. Average cosmogenic Kr spectra, normalised to ^{83}Kr.*

	Aubrites†	Angrites‡	Stannern§	Nakhla#
$^{78}Kr/^{83}Kr$	0.134 ± 0.009	0.228 ± 0.010	0.179 ± 0.008	0.190 ± 0.007
$^{80}Kr/^{83}Kr$	0.565 ± 0.037	0.588 ± 0.030	0.495 ± 0.020	–
$^{82}Kr/^{83}Kr$	0.766 ± 0.033	0.796 ± 0.021	0.765 ± 0.025	0.78 ± 0.02
$^{84}Kr/^{83}Kr$	0.81 ± 0.13	0.46 ± 0.08	0.63 ± 0.17	0.46 ± 0.08
$^{86}Kr/^{83}Kr$	≡0.0075 ± 0.0075	≡0.0075 ± 0.0075	≡0	≡0

Ratios for other achondrites, determined for the eucrite Stannern and Nakhla are given for comparison.
*Determination by (1) extrapolation of the data points for the respective samples, Q, and air towards the adopted $(^{86}Kr/^{83}Kr)_{cosm}$ ratio of 00075 ± 0.0075 and (2) subtraction of the appropriate trapped Kr composition†,‡. The uncertainties cover the results of both methods.
†Based on data for Norton County (trapped Kr: air); Cumberland Falls, Shallowater (Q); Mount Egerton, Mayo Belwa (Q + air).
‡Based on data for D'Orbigny + Sahara 99555 (Q + air).
§Marti *et al.* (1966).
#Ott (1988).

TABLE A5. Cosmogenic Xe spectra, normalised to ^{126}Xe, for the different achondrites measured in this work based on the data given in Hohenberg *et al.* (1981).

	Tatahouine	Aubrites	Pasamonte	Pasamonte*	Pasamonte†	Millbillillie	Angrites	Stannern‡	Artificial meteoroid
$^{124}Xe/^{126}Xe$	0.60 ± 0.20	0.61 ± 0.16	0.62 ± 0.09	0.58 ± 0.02	–	0.59 ± 0.23	0.61 ± 0.03	0.59 ± 0.015	0.60–0.70
	1	1	1	1	–	1	1	1	1
$^{128}Xe/^{126}Xe$	1.52 ± 0.57	1.50 ± 0.41	1.48 ± 0.15	1.34 ± 0.04	–	1.55 ± 0.68	1.51 ± 0.08	$1.45^{+0.25}_{-0.12}$	1.14–1.38
$^{129}Xe/^{126}Xe$	1.60 ± 0.65	1.60 ± 0.40	1.60 ± 0.34	–	–	1.60 ± 0.75	1.60 ± 0.32	–	1.17–1.54
$^{130}Xe/^{126}Xe$	0.95 ± 0.44	0.89 ± 0.30	0.82 ± 0.05	0.73 ± 0.04	1.05	1.03 ± 0.52	0.91 ± 0.07	$0.97^{+0.5}_{-0.25}$	0.70–0.89
$^{131}Xe/^{126}Xe$	3.70 ± 1.54	3.55 ± 1.05	3.40 ± 0.25	2.76 ± 0.15	5.2	3.87 ± 1.82	3.60 ± 0.23	$3.9^{+2.5}_{-1.1}$	1.31–2.16
$^{132}Xe/^{126}Xe$	0.81 ± 0.37	0.76 ± 0.25	0.70 ± 0.04	0.08 ± 0.15	0.80	0.87 ± 0.44	0.78 ± 0.06	$0.9^{+2.3}_{-0.9}$	0.56–0.79
$^{134}Xe/^{126}Xe$	0.052 ± 0.026	0.049 ± 0.019	0.045 ± 0.009	–	–	0.056 ± 0.031	0.050 ± 0.011	≤0.25	0.037–0.053
$^{136}Xe/^{126}Xe$	0.004 ± 0.004	0.004 ± 0.004	0.003 ± 0.003	–	–	0.004 ± 0.005	0.004 ± 0.004	0	–

The Ba and REE concentrations to calculate the spectra are given in Table A6. For comparison, spectra for Pasamonte and Stannern are given. The last column shows the range of Xe isotopic ratios measured in Ba-glass targets within artificial stony meteoroids (5–25 cm radius) irradiated with 600 keV protons (Mathew *et al.*, 1994).
*"Preferred values", Hohenberg *et al.* (1967).
†Pepin and Phinney (1978).
‡Marti *et al.* (1966).

TABLE A6. Average Ba, La, Ce, and Nd concentrations in the achondrites discussed in this work, based mostly on data from whole-rock samples (see last column for references).

Sample	Ba (μg/g)	La (μg/g)	Ce (μg/g)	Nd (μg/g)	Samples used for average	References
Tatahouine*	0.049 ± 0.021†	0.0031 ± 0.0007	0.0081 ± 0.0015	0.0045 ± 0.0009	Tatahouine	Wolf *et al.* (1983); Barrat *et al.* (1999).
Lodranites	7.1 ± 1.8	0.086 ± 0.018	0.31 ± 0.08	0.32 ± 0.06	EET 84302, Gibson, LEW 88280, Lodran (silicate), MAC 88177, Y-791491, Y-8002, Y-74357	Fukuoka and Kimura (1990); Torigoye *et al.* (1993); Mittlefehldt *et al.* (1996); Weigel *et al.* (1999).
Pasamonte	32.1 ± 1.1	3.13 ± 0.11	8.4 ± 0.3	6.05 ± 0.20	–	Tera *et al.* (1970); Gast *et al.* (1970); McCarthy *et al.* (1973); Wänke *et al.* (1977); Mittlefehldt (1979); Shimizu and Masuda (1982, 1986); Shukolyukov and Begemann (1996b).
Aubrites	3.0 ± 0.7	0.17 ± 0.06	0.80 ± 0.32	0.18 ± 0.05	ALHA78113, Aubres, Bishopville, Khor Temiki, Mayo Belwa, Norton County, Peña Blanca Spring, Shallowater	Moore and Brown (1963); De Laeter and Hosie (1978); Shimizu and Masuda (1981); Wolf *et al.* (1983); Graham and Henderson (1985); Burger *et al.* (1989); Keil *et al.* (1989); Lodders *et al.* (1993) and references therein.
Millbillillie	28 ± 14	1.04 ± 0.21	2.8 ± 0.5	2.37 ± 0.27	–	Burger *et al.* (1989); Makishima and Masuda (1993).
Angrites	48.6 ± 1.3	3.4 ± 0.2	8.9 ± 0.5	6.6 ± 0.5	LEW 86010, LEW 87051, D'Orbigny, Sahara 99555	Mittlefehldt and Lindstrom (1990); Nyquist *et al.* (1994); Warren *et al.* (1995); Kurat *et al.* (2001); Mittlefehldt *et al.* (2002).

The adopted values are used for the calculation of the Xe cosmogenic specta according to Hohenberg *et al.* (1981) as given in Table A5.
*Samples of Tatahouine found 63 years after the first finds show 2–4× larger concentrations (Barrat *et al.*, 1999).
†Calculated with [Ba] = (3.1 ± 1.3) × {[La] + [Ce] + [Nd]}, the factor is estimated from those diogenites with complete data sets: ALHA77256, Johnstown, Y-692, Y-75032; References: Mason and Jarosewich (1971), Masuda and Tanaka (1978), Shimizu and Masuda (1981).
Abbreviations: EET = Elephant Moraine, LEW = Lewis Cliff, MAC = MacAlpine Hills, Y = Yamoto, ALH = Allan Hills.